PHYSICAL REVIEW
LETTERS

VOLUME 6 MARCH 1, 1961 NUMBER 5

HYDRODYNAMICS OF HELIUM II IN ANNULAR GEOMETRY*

P. J. Bendt and T. A. Oliphant
Los Alamos Scientific Laboratory, University of California, Los Alamos, New Mexico
(Received January 23, 1961)

A rotating cylinder of helium II is assumed to contain a uniform array of quantized vortex lines parallel to the axis, each having circulation h/m,[1] where h is Planck's constant and m is the mass of a He^4 atom. The lines move with the container, and the resulting average velocity field simulates solid body rotation. Vinen[2,3] pointed out that if a fine wire (~0.001-in. diameter) were located along the axis of the rotating cylinder, there would be one or more quanta of circulation around the wire, in addition to free vortex lines in the liquid. His experiment showed the circulation around the wire stabilized at one quantum unit, giving the value h/m to within 2%. Further, this circulation constituted a persistent current which remained constant for as long as 100 minutes after rotation of the cylinder stopped. The calculations reported in this Letter indicate that it may be possible to establish persistent currents having circulations 10^3 or more times as large as those observed by Vinen.

We have calculated the free energy for a hypothetical velocity field in a rotating annulus having an inside radius r_1 comparable in size to its outside radius r_2. This field consists of an inside region extending from r_1 to r_a in which the superfluid moves around the center cylinder with a velocity field given by $v_s = K/2\pi r$, where K is the circulation. Since this motion is irrotational, there are no vortex lines in the inside region. The outside region, extending from r_a to r_2, consists of a uniform array of vortex lines simulating solid body rotation. Throughout the annulus the normal fluid rotates with the container.

We have written classical expressions for the energy E and angular momentum L of the superfluid motion. In these expressions, we restricted the velocity field of each quantized vortex line to a circle of radius b, determined by letting $\pi b^2 = N^{-1}$, where $N = 2\omega/(h/m)$ is the density of vortex lines.

In this velocity field there are boundaries at r_1, r_a, and r_2. At r_2 the average tangential velocity is that of the annulus, ωr_2. At r_1 the liquid is always sliding past the inside wall. Kuper[4] has suggested that a layer of vortex lines close to the wall, oriented parallel to the cylindrical axis, will provide the necessary slip plane. Ideally these lines will move tangentially along the wall.[5] If they peel off into the bulk of the liquid, they will move across the inside region under the Magnus force.

Two calculations were performed. In the first, the value for K was determined by the criterion that there should be no discontinuity in the average tangential velocity at r_a. The expression for the free energy $F = E - \omega L$ was minimized by setting $\partial F/\partial r_a = 0$. For all values of ω, the value of r_a which corresponds to minimum free energy is larger than r_1, which shows that filling the annulus with a uniform array of vortex lines does <u>not</u> give the lowest free energy. However, still lower free energies than given by the first calculation are obtained if the boundary condition at r_a is ignored. (It may be possible to dispose of the mathematical discontinuity in the average tangential velocity at r_a by locally adjusting the density of vortex lines.) In the second calcula-

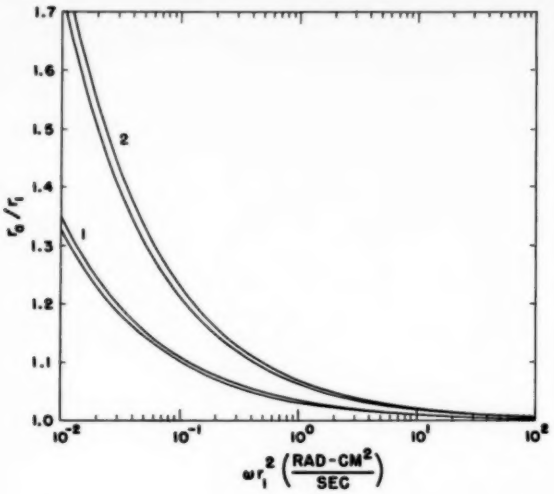

FIG. 1. The ratio r_a/r_1 for minimum free energy in a rotating annulus, plotted against ωr_1^2. The labels 1 and 2 refer to the first and second calculations.

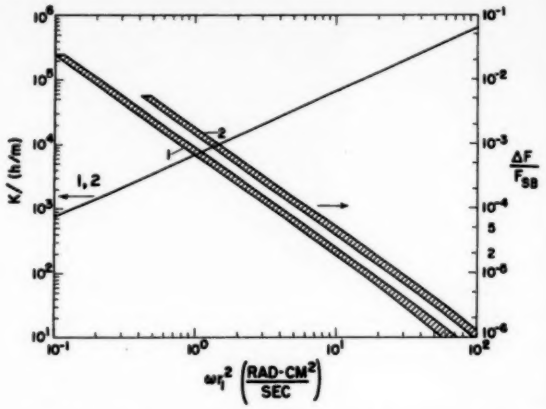

FIG. 2. The circulation K about the center cylinder in units of h/m for minimum free energy, and $\Delta F/F_{sb}$ for $r_2/r_1 = 1.1$. The labels 1 and 2 refer to the first and second calculations.

tion, the free energy was obtained by a double variation with respect both to K and to r_a.

The results are functions of $(h/m)\ln(b/a)/2\pi\omega r_1^2$, where a, the radius of the vortex line core, is taken to be 6.8 A.[3] The results are plotted in Figs. 1 and 2 as functions of the variable ωr_1^2. We have allowed for variations in $\ln(b/a)$ by plotting bands instead of curves. Each quantity plotted falls within the appropriate band provided $10^{-2} \leq \omega \leq 1$ radian/second, and $1 \leq r_1 \leq 10$ cm. In Fig. 2, $\Delta F/F_{sb} = (F - F_{sb})/F_{sb}$, where F is the minimum free energy and F_{sb} is the free energy for simulated solid body rotation (with vortex lines) throughout the annulus. All free energies were calculated for $r_2/r_1 = 1.1$. $\Delta F/F_{sb}$ is positive because the free energies are negative numbers, $|F| > |F_{sb}|$.

Since the minimum free energy is obtained when there are no vortex lines in the region r_1 to r_a, these calculations suggest that a persistent current may be established by decreasing the angular velocity of a rotating annulus to the value of ω at which r_a becomes equal to r_2. There would then be a velocity field proportional to r^{-1} throughout the annulus, except for a layer of vortex lines close to the walls. The absence of vortex lines in the body of the liquid means that there would be no direct mechanism for mutual friction with the normal fluid. $\Delta F/F_{sb}$ (for $r_2/r_1 = 1.1$) has not been plotted in Fig. 2 for values of ωr_1^2 for which $r_a > r_2$, because under these conditions the motion of the superfluid should be independent of the angular velocity of the annulus. It seems that the rotating annulus could be brought to rest, leaving a persistent current of superfluid as a metastable state.

If the first few layers of helium atoms are attached to the wall, then the number of vortex lines required to provide a slip plane at the inside cylinder of a stationary annulus is $K/(h/m)$, and the same number will be needed at the outside wall. It is consistent with the r^{-1} velocity field, the linear dependence of circumference on radius, and the tendency of vortex lines to form closed loops, to have the same number of vortex lines lying radially along the top and bottom liquid surfaces. It is hypothesized, therefore, that each vortex line will comprise an approximately rectangular loop, lying in a plane which contains the cylindrical axis. Such a configuration would permit the irrotational motion inside the boundary layer to flow without dissipation. In the process of stopping the annulus, transient effects may be generated at the walls which dissipate some of the energy of the superfluid motion. To prevent further dissipation of hydrodynamic energy, v_s relative to the stationary walls must be smaller than the critical velocity for creating thermal excitations. An experiment to look for persistent currents by immersing a "Rayleigh disk"[6] is in progress.

*Work performed under the auspices of the U. S. Atomic Energy Commission.

[1]R. P. Feynman, Progress in Low-Temperature Physics (North-Holland Publishing Company, Amsterdam, 1955), Vol. I, p. 17.

[2]F. W. Vinen, Nature (London) 181, 1524 (1958).

[3]H. E. Hall, Advances in Physics, edited by N. F. Mott (Taylor and Francis, Ltd., London, 1960), Vol. 9, p. 89.

[4]C. G. Kuper, Proceedings of the Seventh International Conference on Low-Temperature Physics (University of Toronto Press, Toronto, 1960), Paper 28-2.

[5]L. M. Milne-Thomson, Theoretical Hydrodynamics (MacMillan Company, New York, 1955), 3rd ed., p. 345.

[6]J. R. Pellam, Phys. Rev. Letters 5, 189 (1960); T. R. Koehler and J. R. Pellam, Proceedings of the Seventh International Conference on Low-Temperature Physics (University of Toronto Press, Toronto, 1960), Paper 19-2.

GENERATION AND MEASUREMENT OF HIGHLY IONIZED QUIESCENT PLASMAS IN STEADY STATE

R. C. Knechtli and J. Y. Wada
Hughes Research Laboratories, Malibu, California
(Received January 23, 1961)

The purpose of the experiments described in this Letter is to perfect techniques for generating highly ionized quiescent plasmas of useful density in steady state, and to use such plasmas for a systematic and conclusive investigation of the properties of fully ionized quiescent plasmas. Thermionic electron emission combined with resonance ionization (or contact ionization) of cesium vapor is a most suitable process for producing plasmas of this type. This technique was recognized a number of years ago[1]; more recently, it has found new favor in a number of laboratories.[2-5] The experimental results obtained to date in our Laboratory by means of this technique are summarized below and will be reported more extensively at a later date in papers under preparation.

A quiescent highly ionized cesium plasma is generated and sustained in steady state in the apparatus sketched on Fig. 1. This apparatus consists of two plasma emitters facing one another and immersed in a homogeneous axial dc magnetic field (shown by H_0 on Fig. 1). Each plasma emitter consists of a tungsten plate heated to thermionic emission temperature by electron bombardment from an auxiliary cathode. The whole device, including the hot tungsten plates, is placed in a vacuum-tight and thoroughly outgassed enclosure. The pressure of background gases different from cesium vapor is kept at all times of the order of 10^{-8} mm of Hg or less, in order to keep the effect of these gases negligible. The cesium vapor pressure is controlled by admitting an excess of cesium metal into the apparatus, and accurately controlling the temperature of the enclosure walls. A direct measurement of the cesium vapor pressure by means of saturation ion emission from a hot tungsten filament indicated that this method of control of cesium vapor pressure is, with due care, quite reliable.

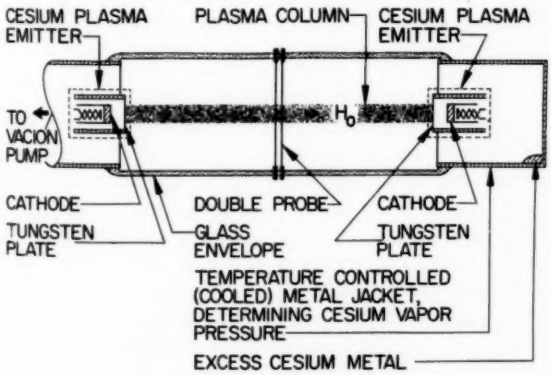

FIG. 1. Apparatus for generation of a highly ionized cesium plasma column in a homogeneous dc magnetic field H_0.

In the apparatus of Fig. 1, ions are emitted by contact ionization of the cesium on the hot tungsten plates; electrons are emitted thermionically on the central hot part of the tungsten plates. Plasma thus is continuously generated at both ends of the plasma column at a rate controlled by the neutral cesium vapor pressure. A relatively modest dc magnetic field (of the order of a few hundred oersteds) is found sufficient to make plasma diffusion in the radial direction negligible. This technique results in a well-defined quiescent cesium plasma column, as indicated in Fig. 1. The first-order cause for plasma loss in this plasma column is volume recombination, together with plasma loss on the small probes used to measure the plasma density and temperature. (The plasma loss on the probes

is readily taken into account and its effect on the degree of ionization of the plasma is, to a first order approximation, independent of plasma density.) The degree of ionization of the plasma then is determined by the condition that the rate of cesium ion generation on the plasma emitters be equal to the rate of cesium ion loss by volume recombination and on the probes. The rate of volume recombination being, by definition, proportional to the recombination coefficient, the latter is found directly from the measurement of the degree of ionization as a function of plasma density.

By means of such a plasma, in an apparatus of the type sketched on Fig. 1, the following experimental results have been obtained:

(a) Validity of double-probe measurements in dc magnetic field. Because of its simplicity, the double-probe method of measurement of plasma density and temperature has been used. Because of the presence of a dc magnetic field, the validity and interpretation of this method of measurement could be subject to question. Our experimental results did, however, substantiate our theoretical expectation that double-probe measurements, even in the presence of a dc magnetic field, are completely reliable under the conditions of our measurements (probe dimensions, spacing, and sheath thickness small compared to the ion cyclotron radius). Comparison of the double-probe measurements of plasma density with microwave cavity plasma density measurements showed excellent agreement (within 30%) over the whole range of magnetic fields investigated (300 to 1500 oersteds). Comparison of the plasma electron temperature evaluated by double probes in the same magnetic fields with pyrometric measurements of the plasma emitter temperature (hot tungsten plates) showed agreement within 10% to 15%. Prior comparison of the plasma electron temperatures with the plasma emitter temperature by measurements of the mean electron cyclotron radius had shown these two temperatures to be the same within measuring accuracy for the conditions of our experiments.[6] We thus conclude that, within the limits stated above, double-probe measurements of both plasma density and temperature in the presence of a magnetic field remain reliable and are not appreciably affected by the presence of the magnetic field.

(b) Plasma diffusion and profile of plasma columns. For a preliminary estimate of the profile of the plasma column and of the nature of diffusion of a quiescent plasma in a dc magnetic field, the apparatus of Fig. 1 was used with only one plasma emitter operating, the other being kept cold. The orientation of the dc magnetic field was then continuously changed so as to sweep the plasma column across the probes (3 fixed probes at different radial positions were used in this experiment). Recording of the plasma density measured by the probes as a function of magnetic field orientation yielded the well-defined profile shown on Fig. 2 for the plasma column. Although more detailed and extensive measurements now being prepared are needed to reach final conclusions, preliminary indications are that plasma diffusion is purely ambipolar, even in the presence of the dc magnetic field. This seems consistent with the results obtained independently and at about the same time as ours by Rynn and D'Angelo.[5]

(c) Measurement of degree of ionization. The results of a typical set of measurements of cesium plasma density and neutral cesium density are shown in Fig. 3. The corresponding values of the degree of ionization ν of the plasma are shown on the same figure. It may be observed that up to a density higher than $n_+ = 10^{12}$ ions/cm^3 a plasma with a degree of ionization

$$\nu = 90\%$$

has been obtained. It is particularly interesting

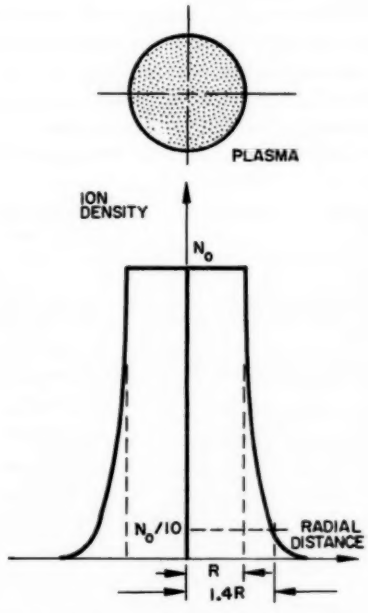

FIG. 2. Profile of cesium plasma column.

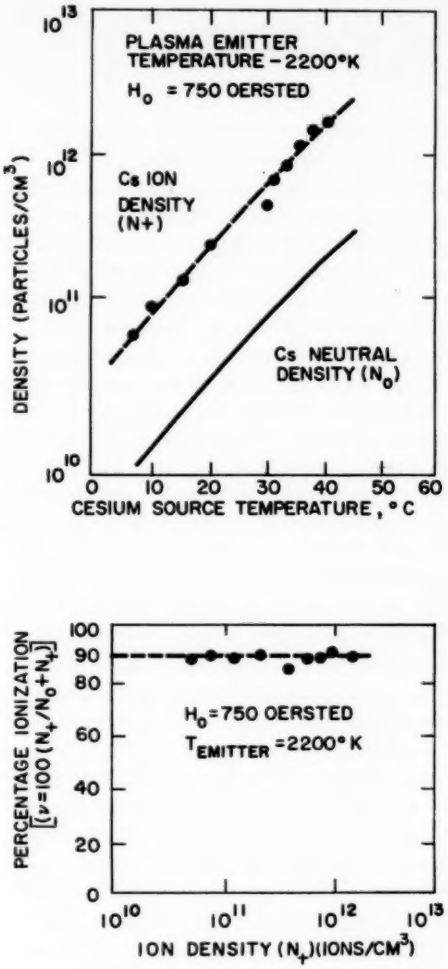

FIG. 3. Ion density, neutral density, and degree of ionization in cesium plasma column.

to mention that the value $\nu = 90\%$ corresponds rather well to the degree of ionization expected from the plasma loss on the probes as long as volume recombination is negligible.

(d) Estimate of recombination coefficient. From the data of Fig. 3 it follows that volume recombination is negligible up to plasma densities exceeding 10^{12} ions/cm^3. This, together with the known dimensions of the plasma column (length $L = 10$ cm), leads to the following upper limit for the recombination coefficient:

$$\alpha < 10^{-10} \text{ cm}^3 \text{ sec}^{-1}.$$

This value is substantially lower than the values reported to date in the literature.[7,8] Our result, however, is not too surprising because of the low probability of formation of molecular ions leading to dissociative recombination. A determination of the actual value of α rather than of its upper limit requires measurements at higher plasma densities, in the apparatus of Fig. 1. This apparatus is presently being modified to make such measurements possible. It will be interesting to observe how close the actual value of α is to radiative recombination. Alternatively, our experiments may provide a verification of the theory recently proposed by D'Angelo[9] for the electron-ion recombination in highly ionized plasmas. It may also be observed that because of the apparently very low value of α, it is reasonable to expect to be able to generate highly ionized quiescent plasmas in steady state by the type of apparatus shown on Fig. 1 up to densities of the order of 10^{14} electrons and ions/cm^3 over appreciable volumes and even higher densities over small volumes.

In conclusion it may be stated that we have demonstrated the usefulness of a very simple technique for generating highly ionized quiescent plasmas in steady state up to relatively high densities, that we have verified the validity of double-probe measurements in the presence of dc magnetic fields, that we have found preliminary evidence that the diffusion of quiescent plasmas in homogeneous dc magnetic fields appears purely ambipolar, that we have established a direct technique for the measurement of the recombination coefficient of cesium plasmas, and that we have found so far this coefficient to be below 10^{-10} cm^3 sec^{-1}.

[1]R. C. Knechtli and W. Knauer, Bull. Am. Phys. Soc. 3, 81 (1958).

[2]R. C. Knechtli and J. Wada, Bull. Am. Phys. Soc. 5, 366 (1960).

[3]R. B. Hall and G. Bekefi, Bull. Am. Phys. Soc. 5, 314 (1960).

[4]G. S. Kino, LMSD Fifth Annual Symposium, December, 1960 (unpublished).

[5]N. Rynn and N. D'Angelo, Second Annual Meeting of the Division of Plasma Physics of the American Physical Society, November, 1960, Paper D4.

[6]W. Knauer (private communication).

[7]F. L. Mohler, J. Research Natl. Bur. Standards 19, 447 (1937).

[8]P. Dandurand and R. B. Holt, Phys. Rev. 82, 278, 819 (1951).

[9]N. D'Angelo, Second Annual Meeting of the Division of Plasma Physics of the American Physical Society, November, 1960, Paper E9.

INFLUENCE OF SPIN ON ELECTRONIC TRANSFORMATIONS*

K. A. Gschneidner, Jr., R. R. McDonald, and R. O. Elliott
Los Alamos Scientific Laboratory, University of California, Los Alamos, New Mexico
(Received February 6, 1961)

Cerium, the first member of the 4*f* transition elements, undergoes a transformation of its electron configuration at atmospheric pressure and about 120°K, or at room temperature and about 7500 atm. We have now shown that this transition is strongly affected by unpaired spins.

It can be shown from considerations of metallic radii and magnetic properties that this transformation involves the promotion of about 0.5 electron per atom from the 4*f* level to the valence band. The room temperature form of cerium, which we will designate as γ, is face-centered cubic and has a lattice constant of about 5.16 A. γ-Ce at standard pressure and temperature has (0.9 ± 0.1) 4*f* electron, or a valence of 3.1 ± 0.1. The low-temperature (or high-pressure) form, which we will designate as α, is also face-centered cubic but has a lattice constant of about 4.85 A. Similar considerations of magnetic data and metallic radii indicate that α-Ce has 0.4 ± 0.1 4*f* electron, or a valence of 3.6 ± 0.1. β-Ce, which can form only on cooling γ-Ce to about 260°K, is hexagonal with $a = 3.68$ A and $c = 11.92$ A and has approximately the same number of valence and 4*f* electrons as γ-Ce. β-Ce is important in connection with the $\alpha \rightleftarrows \gamma$ transformation because it will form from γ-Ce upon cooling and will not transform to α above 50°K. Thus, the amount of α-Ce present at 50°K will be less, by the amount of β-Ce that is formed, than would normally be expected.

The elements that follow cerium do not appear to undergo a transformation of electron configuration similar to that of cerium, except possibly ytterbium, which may transform at a pressure of about 60 000 atm. Presumably the absence of a $4f \rightleftarrows$ valence band electronic transformation in the elements following cerium is due to a large difference in energy between the 4*f* level and valence band. There are, however, two interesting characteristics of these 4*f* transition elements. (1) They exhibit a small decrease in their metallic radii as the atomic number increases; this is known as the lanthanide contraction. (2) They are either strongly paramagnetic or ferromagnetic and have high magnetic moments, which arise from the number of unpaired 4*f* electrons (except the end number, lutetium, which has fourteen 4*f* electrons, i.e., the 4*f* band is completely filled).

Because the $\gamma \rightleftarrows \alpha$ transformation in cerium is electronic in nature and involves large volume changes (more than 15%), this transformation might be influenced (1) by the magnetic field from a magnetic impurity, or (2) by spin-spin interactions between the 4*f* electron of cerium and the magnetic electrons from a magnetic impurity, or (3) by the size of the impurity atom. A consideration of simple alloying theory indicated that probably all of the rare earth metals, some of the actinide metals, and calcium, indium, magnesium, scandium, and sodium might form extensive solid solution alloys; that is, at least 5 atomic percent of any of these elements would be expected to be soluble in cerium. It would seem, then, that the rare earth metals are ideal solute materials for use in investigating the three points mentioned above.

The $\gamma \rightarrow \alpha$ transformation temperatures of cerium alloys containing 2 at. % of the various rare earth metals are shown in Fig. 1. The transition temperature for our cerium stock is 106 ± 5°K. The data shown in Fig. 1 indicate that a 2 at. % addition of all of the solutes except thulium, ytterbium, and lutetium lower the transition temperature of cerium. In Fig. 2, several possible theoretical curves are shown that may be related to the depression of the $\gamma \rightarrow \alpha$ transformation temperature. A comparison of the curve in Fig. 1 with the curve representing the magnetic moments in Fig. 2 shows that the depression is definitely not related to the dipole moment of the magnetic impurity atom. If it were, we would expect that dysprosium and holmium, instead of gadolinium, would have the greatest effect in depressing the temperature, and that samarium would depress the temperature only a few degrees instead of 17°K. On the other hand, the relationship between the "spin only" curve in Fig. 2 and the experimental data is very good. The metals in the latter half of the series (terbium through lutetium) do not seem to have as great an effect on depressing the transformation temperature as do the metals from the first half of the series (lanthanum through europium), which have the same number of unpaired 4*f* electrons. For example,

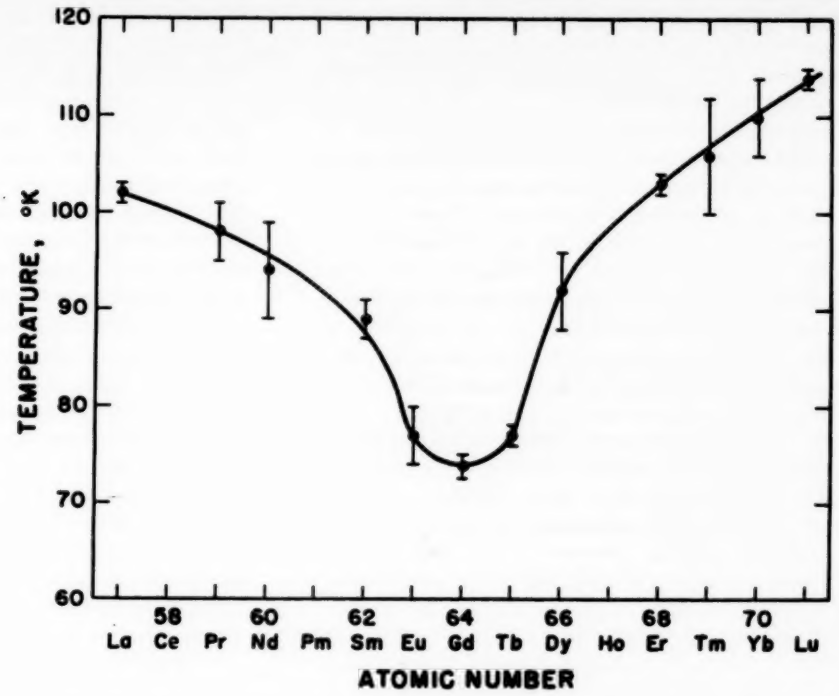

FIG. 1. Influence of 2 at. % rare earth additions on the $\gamma \rightarrow \alpha$ cerium transformation temperature.

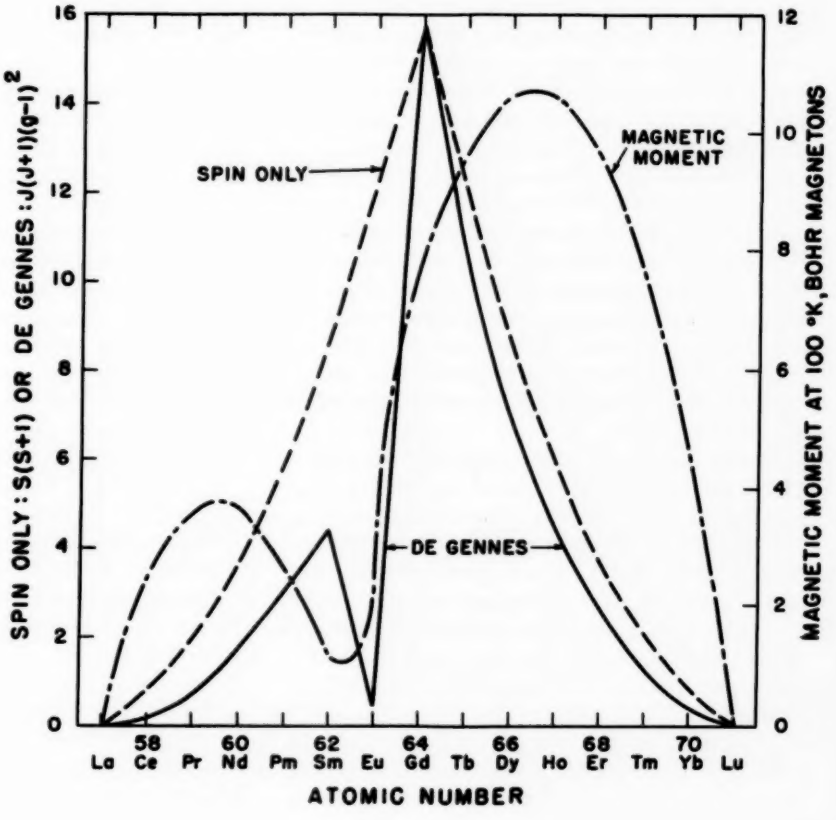

FIG. 2. The magnetic moment, spin only curve, and de Gennes curve, as a function of the atomic number of the rare earth elements.

neodymium with 3 unpaired $4f$ electrons lowers the transformation temperature 12°K, while erbium, which also has 3 unpaired $4f$ electrons, lowers the temperature by only 3°K. This unsymmetrical form of the curve shown in Fig. 1 may be due to other factors which simultaneously, along with the spin of the solute atom, influence the transition temperature. These other factors, which play a minor but noticeable role, might be the size and/or the magnetic moment of the solute atom. The third curve, labeled as "de Gennes" in Fig. 2, is a plot of $J(J+1)(g-1)^2$ versus the atomic number. The term $J(J+1)(g-1)^2$ is from a theoretical proposal, made by de Gennes,[1] concerning the proportionality of the Curie points of the heavy rare earth metals (gadolinium through thulium). Suhl and Matthias[2,3] proposed independently that it is also related to the proportionality of the depression of the superconducting transition temperatures of lanthanum alloys containing 1 at. % rare earth additions. It should be noted in Fig. 2 that the de Gennes curve closely follows the "spin only" curve, except for europium, which, in de Gennes' case, should have little or no effect on the transition temperature. Our experimental results, however, indicate that europium fits the "spin only" curve. An objection might be made on the basis that europium behaves as a divalent solute in cerium and, therefore, it might be expected to lower the transition temperature by the same amount as does gadolinium. X-ray analysis of the 2 at. % europium-cerium alloy, however, shows that the lattice constant of the alloy is smaller than that of pure cerium, and indicates that europium is trivalent in this alloy. If europium were divalent, the lattice constant of the alloy would be expected to be larger than that of pure cerium. Similarly, we have found that ytterbium behaves as a trivalent solute in cerium-rich solid solutions.

In cerium alloys containing 2 at. % rare earth metals, the dependence of the $\gamma \rightarrow \alpha$ transformation temperature on the number of unpaired $4f$ electrons of the rare earth solutes is similar to the dependence of the superconducting transition temperature on the number of unpaired $4f$ electrons of the solute atoms in lanthanum alloys containing 1 at. % rare earth additions. This suggests that the mechanisms involved in both cases are similar. For the lanthanum alloys, Suhl and Matthias[2,3] have proposed an s-f interaction to explain the observed behavior. We believe that the dominant mechanism in the cerium alloys is an indirect f-f interaction via conduction electrons, and that the larger the $4f$ contribution from the solute atom (i.e., the greater the number of unpaired $4f$ electrons) the lower the transition temperature.

We have also examined these same cerium alloys at high pressures and have found that all of the rare earth solutes raise the transformation pressure, but only in proportion to their size. That is, for constant compositions, the larger the size of the solute atom the greater the elevation of the transformation pressure. If the number of unpaired $4f$ electrons has any effect at room temperature and high pressure, it is so small that we were unable to detect it.

In summary we wish to reiterate that the transformation of electron configuration in cerium-rich alloys at low temperatures is dependent upon the number of unpaired $4f$ electrons of the solute atom, and that this phenomenon is similar to (1) the depression of the superconducting transition temperature of lanthanum-rich alloys by rare earth solutes,[3,4] (2) the variation in the Curie points of the rare earth AB_2 Laves phase compounds (A = a rare earth and B = ruthenium, osmium, or iridium),[5] and (3) the variation in the Curie points of the heavy rare earth metals.[1]

*Work performed under the auspices of the U. S. Atomic Energy Commission.

[1]P. G. de Gennes, Compt. rend. 247, 1836 (1958).

[2]H. Suhl and B. T. Matthias, Phys. Rev. 114, 977 (1959).

[3]B. T. Matthias, H. Suhl, and E. Corenzwit, J. Phys. Chem. Solids 13, 156 (1960).

[4]B. T. Matthias, H. Suhl, and E. Corenzwit, Phys. Rev. Letters 1, 92 (1958).

[5]R. M. Bozorth, B. T. Matthias, H. Suhl, E. Corenzwit, and D. D. Davis, Phys. Rev. 115, 1595 (1959).

LARGE ANISOTROPIC KNIGHT SHIFTS IN INTERMETALLIC COMPOUNDS*

R. G. Barnes, W. H. Jones, Jr.,† and T. P. Graham
Institute for Atomic Research and Department of Physics, Iowa State University, Ames, Iowa
(Received January 23, 1961)

A variety of intermetallic compounds having electrical properties like those of a metal might be expected to exhibit anisotropy of the Knight shift of the nuclear magnetic resonance of component nuclei. This class of compounds will include those crystallizing with hexagonal or lower symmetry and in addition those crystallizing with cubic symmetry but possessing atoms at sites of less-than-cubic symmetry. Since the nuclei of most of the metals possess electric quadrupole moments, some interference from quadrupole coupling effects may be expected in these situations. In the case of the pure metals, anisotropic Knight shifts have been reported only for cadmium,[1] tin,[2] and thallium,[3] for all of which the nuclear spin is one-half, thereby precluding quadrupolar effects. When both effects are present, the resonance line shape must be investigated as a function of magnetic field strength to determine the individual contributions. This is especially important if the nuclear quadrupole coupling is large enough to give rise to second-order effects.

The cubic Laves phase compounds of the $MgCu_2$ (AB_2) type provide an excellent example of the latter variety mentioned above. In this structure,[4] the Cu or B atoms occupy sites having only axial symmetry, D_{3d}-$\bar{3}m$. The Mg or A atoms are in positions of cubic symmetry, T_d-$\bar{4}3m$. This structure is one of a number in which the average coordination number is $13\frac{1}{3}$, and the compounds exhibit excellent metallic properties except for their brittleness.

In the course of studying the nuclear quadrupole interaction of the B nuclei in cubic Laves phase compounds,[5] we have also observed examples of large anisotropic Knight shifts. With one exception ($MgCu_2$ itself), the observed resonance line shape results from an interplay of the anisotropic Knight shift with the second-order nuclear quadrupole interaction. In a powder sample, each of these effects gives rise to a characteristic line shape.[6] These shapes are, however, qualitatively somewhat similar, so that if the quadrupole interaction is the major effect, the resonance line shape is not significantly altered from that of the quadrupole interaction alone. In the absence of anisotropic Knight-shift broadening, the splitting $\Delta\nu$ between derivative maxima of the $\frac{1}{2} \leftrightarrow -\frac{1}{2}$ transition caused by the nuclear quadrupole interaction in second order is given by[7]

$$\Delta\nu = b/\nu + \sigma, \tag{1}$$

provided that $\sigma \lesssim 0.2\, b/\nu$. Here $b = (25/64)(2I+3) \times e^4q^2Q^2/4I^2(2I-1)h^2$, where e^2qQ/h is the quadrupole coupling in Mc/sec, and 2σ is the linewidth based on the Gaussian shape approximation. For nonconductors, a plot of $\Delta\nu$ vs $(1/\nu)$ yields a straight line from which b and σ may be determined. If anisotropic Knight shift broadening also occurs, the observed $\Delta\nu$ may be represented to a first approximation by

$$\Delta\nu = b/\nu + a\nu + \sigma. \tag{2}$$

In this expression, $a\nu = \Delta\nu_{\parallel} - \Delta\nu_{\perp} = 3\nu\delta_{ax}$, and gives the contribution of the anisotropic Knight shift to the linewidth.[3] For the cases studied here, $\sigma < b/\nu$ or $\sigma < a\nu$, whichever is the more important contribution to $\Delta\nu$ at low or high frequencies. Neglecting σ leads to

$$\nu\Delta\nu = b + a\nu^2, \tag{3}$$

so that $\nu\Delta\nu$ should be linearly proportional to ν^2.

A striking example of this behavior is provided by the Al^{27} resonance in $TmAl_2$. The measured values of the splitting $\Delta\nu$ are shown by the data points in Fig. 1(a), and a plot of the quantity $\nu\Delta\nu$ vs ν^2 for these data is shown in Fig. 1(b), in which the straight line is a least-squares fit of (3) to the points. From this, the nuclear quadrupole coupling and the parameter a are found to be $e^2qQ/h = 3.05$ Mc/sec and $a = 0.0061$. The solid curved line in Fig. 1(a) is drawn using these parameters.

We have also observed the anisotropic Knight shift contribution to the splitting $\Delta\nu$ of the Al^{27} resonance in $CaAl_2$ and $YbAl_2$ which have smaller nuclear quadrupole couplings[5] than $TmAl_2$. In the cases of $LaAl_2$ and $CeAl_2$, this contribution to the splitting is not detected. For these, the quadrupole coupling is approximately 4.5 Mc/sec; hence b/ν is presumably still larger than $a\nu$ at the highest frequency at which observations were made. The Cu^{63} and Cu^{65} resonances in the prototype compound $MgCu_2$ also display anisotropic Knight shift broadening. However, in this case, the quadrupole coupling is so small that the ob-

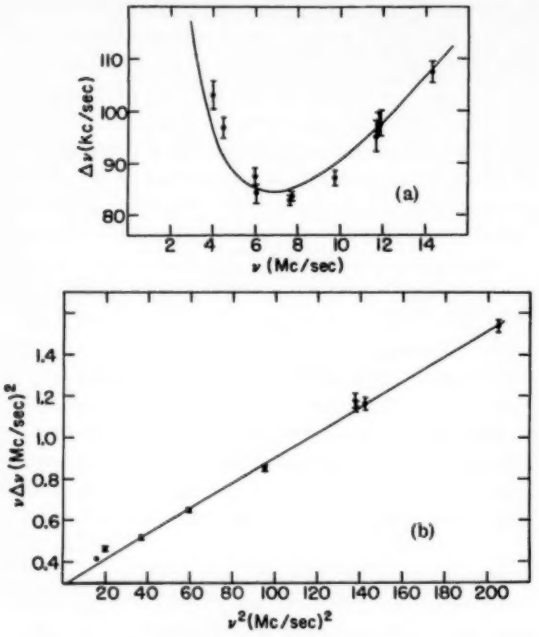

FIG. 1. (a) Resonance linewidth (separation between derivative maxima) as a function of resonance frequency for the Al^{27} resonance in $TmAl_2$. The solid curved line is the straight line of Fig. 1(b). (b) The product $\nu\Delta\nu$ for the data points of Fig. 1(a) as a function of the square of the resonance frequency. The solid line is the least-squares fit of Eq. (3) to the data points.

served splitting is dominated by the anisotropic Knight shift over virtually the entire range of observation.

These experimental results are summarized in Table I. Values of the quantities b/ν and $a\nu$ are given at two resonance frequencies, 4 and 16 Mc/sec. The Van Vleck[8] nuclear dipolar half-linewidth σ (Gaussian approximation) is included for comparison. In addition, the isotropic and axial components, δ_{iso} and δ_{ax}, of the Knight shift tensor[3] and the quadrupole coupling derived from the parameters a and b of Eq. (3) are also given. Besides augmenting the relatively few examples of anisotropic Knight shifts, these results are interesting because they suggest that, in general, several factors combine to cause anisotropy of the shift in the Laves phase compounds. In the cases of $MgCu_2$, $CaAl_2$, and $YbAl_2$, which presumably do not possess ions having unpaired d or f electrons, anisotropy of the p or d character of the conduction band, or of the electron g factor, or of both, must be responsible for the anisotropic shift. On the other hand, a major part of the large anisotropy in the case of $TmAl_2$ very likely arises from the nonisotropic part of the s-f exchange interaction, the isotropic part of which has been shown by Jaccarino et al.[9] to account for the large Knight shifts in the rare-earth-aluminum compounds.

The authors are indebted to Dr. A. H. Daane for providing the rare-earth metals and to Dr. J. F. Smith and Dr. D. Peterson for preparing the intermetallic compounds used in this work.

*Contribution No. 988. Work was performed in the Ames Laboratory of the U. S. Atomic Energy Commission.

†Present address: International Business Machines Research Laboratories, Owego, New York.

[1]T. J. Rowland, Phys. Rev. 103, 1670 (1956).

[2]N. Bloembergen and T. J. Rowland, Acta Met. 1, 733 (1953).

[3]N. Bloembergen and T. J. Rowland, Phys. Rev. 97, 1679 (1955).

[4]A. E. Dwight, Trans. Am. Soc. Metals 53, 477

Table I. Second-order quadrupole and anisotropic Knight shift linewidth parameters for nuclear magnetic resonances in cubic Laves phase compounds. Results for some pure metals are included for comparison.

Compound and nucleus	b/ν (kc/sec) at 16 Mc/sec	$a\nu$ (kc/sec) at 16 Mc/sec	b/ν (kc/sec) at 4 Mc/sec	$a\nu$ (kc/sec) at 4 Mc/sec	σ (kc/sec)	δ_{iso} %	δ_{ax} %	e^2qQ/h (Mc/sec)
$Mg(Cu^{63})_2$		7.52		1.88	1.97	0.240	0.019	<0.3[a]
$Ca(Al^{27})_2$	9.38	5.70	37.5	1.43	2.15	0.105	0.036	2.19
$Yb(Al^{27})_2$	13.0	6.08	52.0	1.52	2.0	0.110	0.040	2.58
$Tm(Al^{27})_2$	18.1	97.6	72.5	24.4	2.0	-0.55	-0.25	3.05
Cd^{111} [b]						0.415	0.014	
Sn^{117} [c]						0.76	0.013	
Tl^{205} [d]						1.56	0.08	

[a]Estimate based on best fit of data to Eq. (3) in text.
[b]See reference 1.
[c]See reference 2.
[d]See reference 3.

(1960).
[5]W. H. Jones, Jr., T. P. Graham, and R. G. Barnes (to be published).
[6]N. Bloembergen, Report of the Bristol Conference on Defects in Crystalline Solids (The Physical Society, London, 1954), p. 1.
[7]A. H. Silver, J. Chem. Phys. 32, 959 (1960).
[8]J. H. Van Vleck, Phys. Rev. 74, 1168 (1948).
[9]V. Jaccarino, B. T. Matthias, M. Peter, H. Suhl, and J. H. Wernick, Phys. Rev. Letters 5, 251 (1960).

RELAXATION MECHANISMS IN FERROMAGNETIC RESONANCE

T. Kasuya* and R. C. LeCraw
Bell Telephone Laboratories, Murray Hill, New Jersey
(Received January 4, 1961)

Up to the present, the agreement between theory and experiment in ferromagnets for the relaxation time, τ_0, of spin waves with zero wave vector (uniform precession) has not been satisfactory, especially in highly polished samples with narrow linewidths.[1] The purpose of this Letter is to report the most recent observations of τ_0 in yttrium iron garnet (YIG), which has the narrowest known ferromagnetic resonance linewidth, and to outline the essential points of a theory which adequately accounts for these observations. The theory is based on the effects of single-ion anisotropy, or local magnetostriction, in a simplified two-sublattice ferrimagnetic model.

The character of τ_0^{-1} in YIG along the [111] crystal axis is as follows:

(i) The magnitude of τ_0^{-1} is 2.4×10^6 sec^{-1} at room temperature and a frequency of 5.7 kMc/sec.

(ii) τ_0^{-1} is proportional to T^n, where $1<n<2$ in the range 150°K to 400°K with the larger values of n corresponding to higher temperatures.[2] (The behavior or τ_0^{-1} below 150°K in the present samples appears to be determined by additional processes other than those considered here, and will be reported on by E. G. Spencer.)

(iii) τ_0^{-1} at room temperature is proportional to frequency, at least for $\nu \geq 3$ kMc/sec.[3]

(iv) τ_0^{-1} at room temperature is nearly proportional to M_S^{-1}, where M_S is the saturation magnetization. This relation was determined by doping YIG with gallium and aluminum, which substitute primarily on tetrahedral sites, and indium, which substitutes on octahedral sites.[4]

The above observations of τ_0^{-1} have been made possible primarily by the following three developments: (1) elimination of the effects of surface roughness, (2) elimination of rare earth impurities,[5] and (3) separation of spin-spin from spin-lattice relaxation effects. These and other related developments will be discussed in detail in a forthcoming paper. At this time we will briefly describe the technique which was used for most of the data.

Schlömann and Morganthaler have shown[6] that growing pairs of spin waves of equal and opposite wave number and frequency $\omega_p/2$ may be excited when an rf field of frequency ω_p with sufficient magnitude is applied parallel to the dc magnetic field, H_{dc}. The threshold rf field is

$$h_{crit} = \omega_p/(\gamma^2\tau_k 4\pi M_S \sin^2\theta_k), \qquad (1)$$

where θ_k is the angle between $\vec{k}$ and H_{dc}. Thus the threshold is lowest for $\theta_k = \pi/2$. By measuring h_{crit} as a function of H_{dc}, and using the familiar dispersion relation for spin waves, together with the measured value[7] of the exchange constant D, one can obtain a plot of τ_k^{-1} vs k as shown in Fig. 1. A conventional microwave spectrometer with a critically coupled reflection cavity was used for these experiments.

The data in Fig. 1 can be described by

$$1/\tau_k = (1/\tau_0) + Bk, \qquad (2)$$

from $k = 0.35\times10^5$ to 1.55×10^5 cm^{-1}. These data have several important features: (1) τ_0^{-1} obtained by this technique is essentially independent of surface roughness, which is known to affect strongly the ordinary uniform-precession linewidth. Hence τ_0^{-1} must be a property of the bulk material. (2) τ_0^{-1} obtained here is essentially the same as T_{10}^{-1}, the inverse spin-lattice relaxation time of the uniform precession, as measured on the same sample by the frequency modulation technique.[1] (3) For the k numbers involved here, Sparks and Kittel[8] have shown that the k-dependent part of τ_k^{-1} should be linear in k. The observed value of B in Fig. 1 is in approximate agreement with their theory. (The latter point will be considered in more detail separately.)

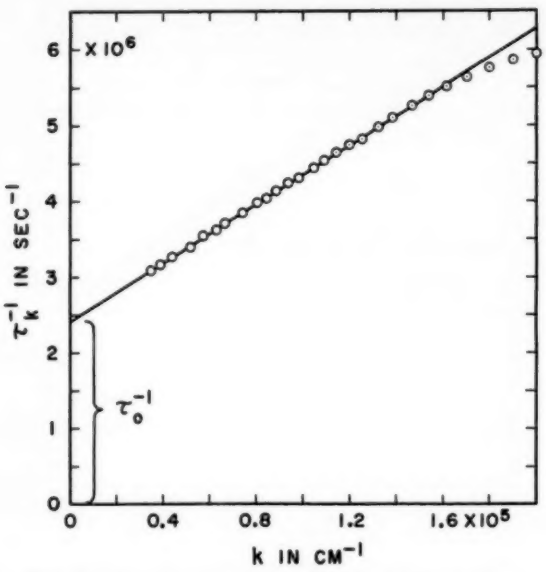

FIG. 1. Room temperature values of τ_k^{-1} vs wave number k for single-crystal YIG along the [111] crystal axis, using the parallel-pump technique and small spherical samples. The pump frequency is 11.4 kMc/sec and the spin-wave frequencies are 5.7 kMc/sec. The departure of the data from the straight line of Eq. (2) is probably due to the assumption $Dk^2 \ll \hbar\omega$, in reference 8, no longer being satisfied.

To explain the above results we have considered the following interactions: dipole, pseudodipole, and single-ion anisotropy, including both uniaxial and cubic terms as found by Geschwind.[9] As mechanisms of relaxation we have considered the following: three magnons, four magnons, one magnon—one phonon, two magnons—one phonon, and one magnon—two phonons. Therefore, there are twenty mechanisms when combined with the above four interaction Hamiltonians.

In this note we cannot give the theoretical details. Our purpose is to describe the important differences between our ferrimagnetic model and previously used ferromagnetic models, and to identify the mechanisms which have been found in detailed calculations to be in order of magnitude agreement with the experiments.

We have used a simplified ferrimagnetic model for YIG with two equivalent sublattices having different quantities of spin in each sublattice, namely $S_A = 5/2$ and $S_B = 5/3$. A ferrimagnetic model was used for the following reasons. Firstly, the spin-wave spectrum, $E(k)$, is considerably different in a ferrimagnet from that in a ferromagnet, with ferrimagnets having both acoustic and optical branches. For the acoustic spin-wave modes, $E(k)$ for the low-lying states is written as Jk^2 in both cases. But for smaller values of $S_A - S_B$, J becomes larger and the range of equivalence becomes smaller. In the larger k range, $E(k)$ should then be replaced by $\hbar u_S k - \Delta$ as in an antiferromagnet, where u_S is the spin-wave velocity and Δ is associated with the energy gap between the acoustic and optical branches. This implies that the state density becomes larger than would be expected by extrapolation from the smaller k range.

In the second place, the amplitude of the spin waves becomes larger than in a simple ferromagnetic model. Also in a ferrimagnetic model a spin operator means one spin quantum up or down in total, but when we consider each sublattice the amplitude becomes larger, for example in the small k range by the factor $[(S_A \text{ or } S_B)/(S_A - S_B)]^{1/2}$. (When $S_A - S_B$ becomes very small, this factor is determined by the anisotropy.) This factor is very important in explaining the M_S^{-1} dependence of τ_0^{-1}. We are considering here relaxation processes of small k spin waves. Thus in cases of long-range mutual spin interactions, such as the dipole type, and interactions with other small k quanta, this fine structure does not have an important effect. Here there is no essential difference between ferro- and ferrimagnetism. But for interactions with large k quanta, the fine structure has an essential effect and the interaction increases by the above factor. In the case of single-spin interactions or short-range interactions this factor does not vanish in interactions with either small or large k spin waves.

Among the twenty mechanisms originally considered, the important interactions are three-magnon processes by dipole, uniaxial, and cubic anisotropies; and two-magnon—one-phonon processes by dipole and uniaxial anisotropy (hereafter referred to as processes I, II, III, IV, and V, respectively). Processes I and III are available to τ_k^{-1} ($k \neq 0$) and II, IV, and V are available to τ_0^{-1}. Concerning τ_k^{-1}, process I was calculated by Sparks and Kittel[8] in a simple ferromagnetic model. We would like to mention briefly the difference obtained with our simple ferrimagnetic model. For k larger than 10^4 cm^{-1} in YIG, interactions with smaller k spin waves are important and the result is the same as that of Sparks and Kittel. For $k < 10^4$ cm^{-1}, however, the fine structure becomes important and τ_k^{-1} is multiplied by the factor $S_A^2/(S_A - S_B)^2$. Process

III is also important for τ_k^{-1}. This process gives the same T, ν, and k dependence as I and also the same order of magnitude, but the M_S dependence is very different, namely $\tau_k^{-1} \sim M_S^{-3} J^{-1}$. Therefore, III would be important in materials with smaller M_S.

To explain the experimental results for τ_0^{-1} in YIG, we have considered in detail processes II, IV, and V. Process IV depends rather sensitively on the crystal structure and energy spectrum, and in some cases (not unreasonable in YIG) it gives the correct T, ν, and M_S^{-1} dependence. However, in order of magnitude it is more than two orders too small. A simple body-centered cubic lattice was assumed for the calculation of IV and although the exact crystal structure is an important factor, we do not expect an increase of two orders of magnitude in other crystal structures. Concerning II and V, the particular character of the uniaxial anisotropy in YIG is highly important in both cases. As is well known, YIG is cubic, and the large local uniaxial anisotropy term when averaged over the unit cell vanishes. The macroscopic magnetostriction is also observed to be small. It is logical then to assume that a large local magnetostriction effect exists which is important in process V.

Because of the above, the only interactions available to process II are those in which the total wave vector of the spin waves and phonons changes by a finite value K; or some types of interband transitions. In process V both types of interactions, $K = 0$ and $K \neq 0$, are available, with the $K = 0$ type probably more important. The $K = 0$ type includes interactions with both acoustic and optical phonons, and it is possible that the interaction with optical phonons is more important than with acoustic phonons.

Detailed calculations show that in process II, τ_0^{-1} is proportional to ν, and nearly M_S^{-1} and T^2. The order of magnitude is also in good agreement. In process V with $K = 0$, τ_0^{-1} is proportional to ν, T, and nearly M_S^{-1}. In order of magnitude, the agreement is good if we take a value of 5 cm^{-1} for the anisotropy constant per unit uniaxial distortion. This value is not unreasonable when compared with values obtained from other experiments. We are led to conclude that processes II and V are probably the dominant processes for the relaxation of τ_0 in YIG at intermediate temperatures, with V being dominant at lower temperatures and II at higher temperatures. The details will be given in full papers.

---

*On leave of absence from the Institute for Solid-State Physics, University of Tokyo, Tokyo, Japan.

[1] τ_0 as used here is the same quantity as T_{10}, the spin-lattice relaxation time of the uniform precession, as defined in R. C. Fletcher, R. C. LeCraw, and E. G. Spencer, Phys. Rev. 117, 955 (1960).

[2] P. Pincus and H. Suhl [Bull. Am. Phys. Soc. 5, 492 (1960)] have reported a larger exponent of T for YIG in this temperature range based on earlier work of one of us (RCL). The value of n given above is now known to be more accurate.

[3] Below ~3 kMc/sec in YIG, additional processes not proportional to ν can contribute to τ_0^{-1}. These have been considered by J. J. Green and E. Schlömann, 1960 Conference on Magnetism and Magnetic Materials (to be published).

[4] M. A. Gilleo and S. Geller, Phys. Rev. 110, 73 (1958).

[5] E. G. Spencer, R. C. LeCraw, and A. M. Clogston, Phys. Rev. Letters 3, 32 (1959).

[6] E. Schlömann, J. J. Green, and U. Milano, J. Appl. Phys. 31, 386S (1960); F. R. Morganthaler, J. Appl. Phys. 31, 95S (1960). Also, F. R. Morganthaler, doctoral thesis proposal, Massachusetts Institute of Technology, 1959 (unpublished).

[7] D. T. Edmonds and R. G. Peterson, Phys. Rev. Letters 2, 499 (1959); 4, 92 (1960). J. E. Kunzler, L. R. Walker, and J. K. Galt, Phys. Rev. 119, 1609 (1960).

[8] M. Sparks and C. Kittel, Phys. Rev. Letters 4, 232 (1960).

[9] S. Geschwind, Phys. Rev. 121, 363 (1961).

EFFECT OF DILUTE SOLID SOLUTIONS OF IRON AND OF NICKEL ON THE NUCLEAR RESONANCE OF Co^{59}†

Richard Conley La Force, S. Frederick Ravitz, and Gene F. Day
Department of Mineral Technology, University of California, Berkeley, California
(Received January 25, 1961)

In 1959 Gossard and Portis observed the first nuclear resonance signals from ferromagnetic Co^{59}, thus initiating a technique particularly suited to the study of the electronic structure of ferromagnets.[1]

In hope of obtaining additional information about the ferromagnetic state, we have studied the nuclear resonance spectra of the Co^{59} matrix in ferromagnetic solid solutions containing small amounts of iron or nickel. The experimental results are displayed in Figs. 1 and 2. In pure cobalt four lines are observed other than the principal resonance from nuclei in the fcc phase at 213.1 Mc/sec. The resonance at 221.3 Mc/sec is produced by nuclei in the hexagonal phase (both hexagonal and fcc phases of cobalt co-exist at room temperature).[2] The other three lines (218.5, 215.6, and 210 Mc/sec) arise through the interaction of nuclei in the fcc phase with stacking faults.[3] This interpretation is supported by the behavior of the spectra upon the addition to the cobalt matrix of iron, which stabilizes the fcc phase. First the line at 221.3 Mc/sec disappears as the concentration of iron is increased; then the other three disappear at slightly higher iron concentrations.

The addition of 1 or 2% iron to the cobalt matrix produces three new resonance lines, two higher in frequency than the pure cobalt resonance (215.6 Mc/sec and 214.2 Mc/sec) and one lower (210.1 Mc/sec).

The intensities of these lines are in the ratio

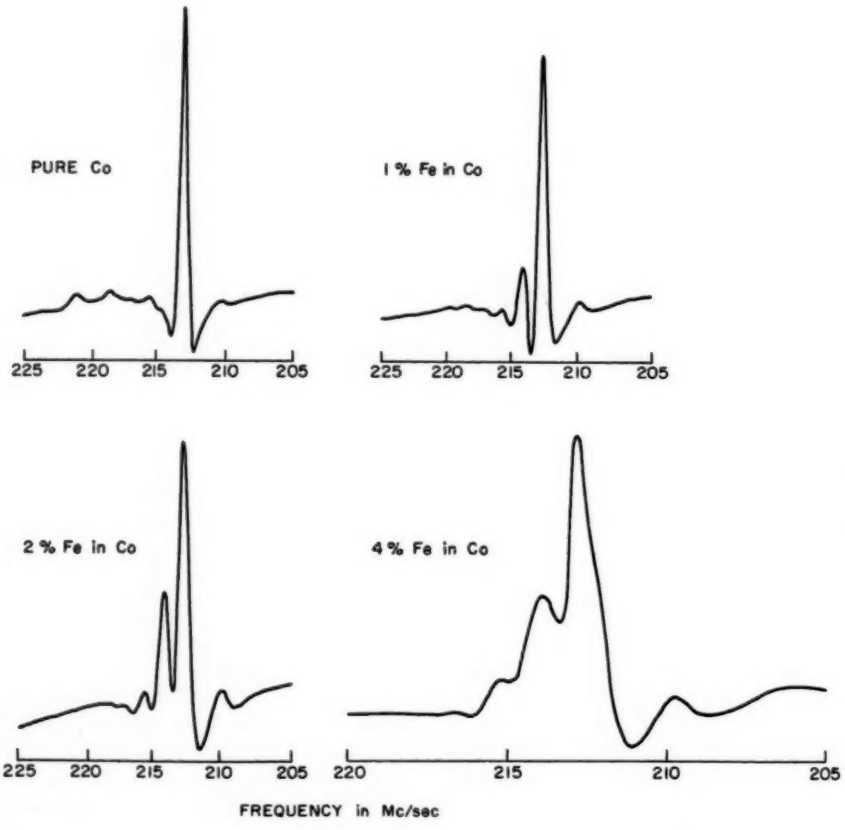

FIG. 1. The first derivative of the Co^{59} nuclear resonance spectra in pure Co and Fe-Co alloys as a function of frequency. The vertical scales are not comparable between spectra.

of 2:1:4 which strongly suggests that they arise from nuclei in shells about an iron impurity (there are twelve nuclei in the first shell, six in the second, and twenty-four in the third).

For the dilute nickel solutions the situation is much the same with respect to the effect of stacking faults and the resonance from the hexagonal phase. Stacking-fault lines are observed at higher concentrations of nickel than of iron, which is reasonable since nickel does not stabilize the fcc phase so well as iron.[4] Co^{59} resonance lines are found at 205, 209.5, 211.1, and 211.8 Mc/sec due to the presence of nickel. There is so much overlap of lines, however, that relative intensity measurements cannot be made as reliably as in the case of iron-cobalt alloys. Although intensity comparisons are difficult to make, we estimate that the total integrated intensity does not change upon alloying.

In trying to understand these results there are two general effects that one must consider. The first is the possibility of a direct interaction between an impurity atom and a nearest neighbor matrix atom. We can obtain some estimate of the size of this interaction from the low-temperature specific heat data.[5] For small concentrations of cobalt in iron the hyperfine field at the cobalt nucleus is increased by about 80 koe. Remembering that there are eight nearest neighbors in the bcc phase and assuming the interaction to be additive leads to an estimate of 10 koe for the effect of an iron atom on a cobalt nearest neighbor. This means that the nearest neighbor line is expected to be about 10 Mc/sec higher in frequency. It is observed 3 Mc/sec lower, however.

The second general effect is the scattering of conduction electrons by an impurity atom to produce a spin polarization about the impurity center. Ruderman and Kittel and later Yosida[6] showed that conduction electrons scattered by a localized spin are thereby spin polarized. The spin polarization is a periodic function of the radial distance from the scattering center and dies out as $1/(rk_f)^3$, where k_f is the value of the quasi-momentum at the Fermi surface. Friedel et al.,[7] considering the possibility of d electrons being in virtual bound states, have shown that in this case also the scattered conduction electrons will be spin polarized, the polarization again dying out as $1/(rk_f)^3$. We should like to point out that the scattering of conduction electrons from a localized charge[8] is sufficient to produce a spin polarization about the scattering

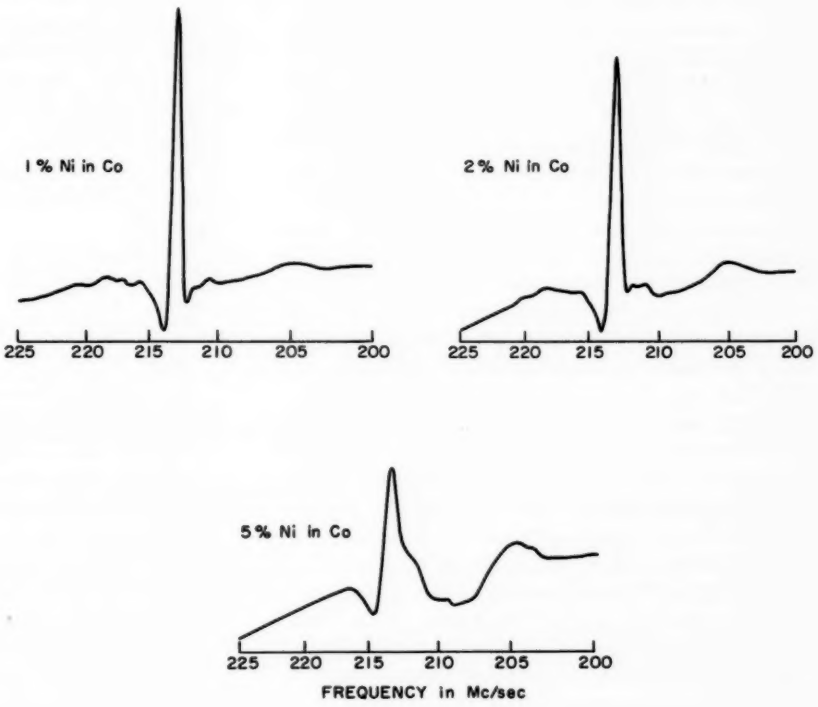

FIG. 2. The first derivative of the Co^{59} nuclear resonance spectra in Ni-Co alloys as a function of frequency. The vertical scales are not comparable between spectra.

center. Charge scattering causes a periodic variation in electron density about the localized charge, but in a ferromagnet this is equivalent to a variation in spin polarization since the conduction electrons are spin polarized through interaction with d electrons.[9] This polarization dies out as $1/(rk_f)^2$ and might therefore be expected to give the largest contribution to the effective magnetic field at distant neighbors.

We have attempted to fit the iron-cobalt alloy data by a combination of a direct interaction acting on the impurity nearest neighbors and charge scattering producing an effective field for all neighbors. We find that the data can be fitted rather well with a value of the quasi-momentum vector halfway to the edge of the first zone and a value of the s - d exchange energy corresponding roughly to the free-atom value.[9] Although the physical situation is not so simple as this, the results are quite encouraging. For the nickel alloys we find that charge scattering would predict the second and third neighbor lines shifted to lower frequency while the nearest neighbor line should be found at higher frequency. Although we cannot make a unique assignment of resonance lines to nuclear positions, we do observe all the lines shifted to lower frequency. This means that the nearest neighbor resonance position is not correctly predicted by scattering alone. But arguing again from the specific heat data,[5] we find that the direct interaction should shift the nearest neighbor line to lower frequencies.

The effect of stacking faults may also be treated as a scattering problem. A stacking fault in fcc Co is a region about 5000 atoms long, perhaps 200 atoms wide, and exactly 2 atoms thick, hexagonally packed. This region appears, so far as the conduction electrons are concerned, as a sheet of material of different propagation constants from the bulk fcc matrix. The interference of the incident and reflected electrons produces a periodic variation in electron density near the stacking fault that dies out inversely with the distance. The relative positions of the stacking fault lines agree qualitatively with the previous assignment of k_f, while the sizes of the frequency shifts are accounted for if the conduction electrons change effective mass by a few percent in crossing the stacking fault boundary.

A more detailed discussion of these various effects together with additional experimental results will be published elsewhere.

It has very recently come to our attention that work similar to ours is being done by Y. Koi and co-workers. We understand that their observations are generally similar to those reported here.[10]

We are pleased to express our thanks to Professor A. M. Portis for many interesting discussions.

---

†This work has been supported in part by the Office of Naval Research and the National Science Foundation.

[1]A. C. Gossard and A. M. Portis, Suppl. J. Appl. Phys. 31, 205S (1960).

[2]Y. Koi, A. Tsujimura, and T. Kushida, J. Phys. Soc. Japan 15, 2100 (1960).

[3]R. Street, D. S. Rodbell, and W. L. Roth, Phys. Rev. 121, 84 (1961); W. Hardy, J. Appl. Phys. (to be published).

[4]M. Hansen, Constitution of Binary Alloys (McGraw-Hill Book Company, Inc., New York, 1958).

[5]V. Arp, D. Edmonds, and R. Petersen, Phys. Rev. Letters 3, 212 (1959).

[6]M. Ruderman and C. Kittel, Phys. Rev. 96, 99 (1954); K. Yosida, Phys. Rev. 106, 893 (1957).

[7]J. Friedel, Advances in Physics, edited by N. F. Mott (Taylor and Francis, Ltd., London, 1954), Vol. 3, p. 446.

[8]W. Kohn and S. H. Vosko, Phys. Rev. 119, 912 (1960); N. Bloembergen and T. J. Rowland, Acta Met. 1, 731 (1953).

[9]W. Marshall, Phys. Rev. 110, 1280 (1958).

[10]Y. Koi, A. Tsujimura, T. Hihara, and T. Kushida, J. Phys. Soc. Japan (to be published).

PION PHOTOPRODUCTION AT BACKWARD ANGLES NEAR THE SECOND NUCLEON-PION RESONANCE*

L. Hand and C. Schaerf
High-Energy Physics Laboratory, Stanford University, Stanford, California
(Received February 7, 1961)

During the past several years there has been much evidence for a resonant $T=1/2$ state in the pion-nucleon interaction at c.m. energy about 320 Mev above the $J=3/2$, $T=3/2$ resonance. The evidence for the second resonance comes from π^--p total cross sections,[1-3] and the photoproduction of single π^+ mesons from hydrogen.[4-6] This Letter describes a photoproduction experiment which confirms differences between the scattering and the photoproduction peaks already inferred from the data of Dixon and Walker at the California Institute of Technology[5] and of the Frascati group.[6]

The peak in the differential cross section for photoproduction at 90° c.m. appears at a photon energy of 680-700 Mev and shows a width[7] of about 150 Mev in the Dixon and Walker data, and 60-70 Mev in the Frascati data which have better photon-energy resolution. The cross section at 20° c.m. measured at Frascati exhibits similar peaks. For the total nucleon-pion scattering cross-section data in the $T=1/2$ state the peak cross section occurs at a pion laboratory kinetic energy of 600 ± 15 Mev,[3] or 605 ± 6 Mev,[2] with a width of 120 Mev. The energy scale of photoproduction experiments is 150 Mev higher than that of the scattering experiments for equal c.m. energies. The total scattering cross-section peak, if plotted at the corresponding photon energies, is thus shifted upwards by 50-70 Mev and is broader than the Frascati photoproduction data would indicate. Walker pointed out[8] that at 180° (and 0°) the contribution to the photoproduction cross section of the meson current term and its interference with other terms is zero. This is characteristic of any term which does not flip the nucleon spin. Dixon and Walker extrapolated their measurements to 180° using a Moravcsik fit[9] to their data at smaller angles. The extrapolated cross section showed no resonant behavior near the second resonance energy.[8]

The present experiment measures with good statistics the photoproduction cross sections under the following two conditions: (a) photon energy 500-820 Mev, laboratory angle 180°; (b) photon energy 500-770 Mev, laboratory angle 135° (i.e., c.m. angle from 149° to 152°). The results are shown in Fig. 1. Estimated resolution functions in photon energy for the two angles are traced in the figure. The broadening of the 135° resolution is caused by the angular variation of the kinematics.

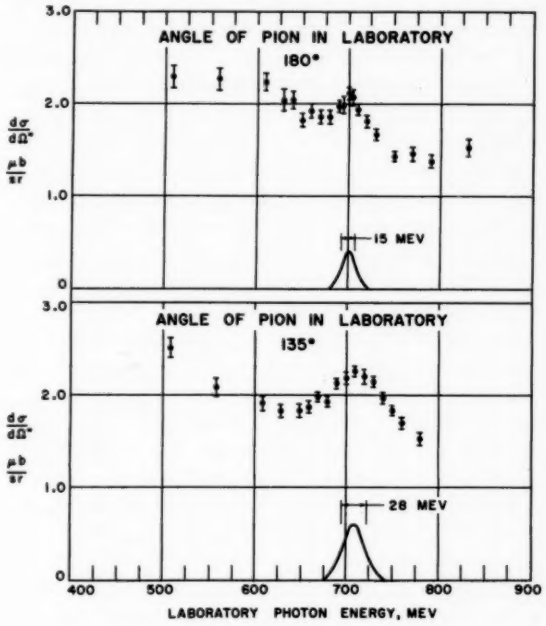

FIG. 1. Differential cross section in the center-of-mass system as a function of photon energy at fixed laboratory angles of the pion. The solid lines indicate the photon energy resolution as calculated from the spectrometer momentum acceptance, the angular variation of the kinematics, and the finite target size.

For the 180° measurements, a beam of 880-Mev electrons from the Mark III linear accelerator struck a 0.052-radiation-length tantalum radiator and was then bent by a small sweeping magnet. The photon beam passed through a $\frac{1}{2}$-in. diameter lead collimator; it then passed through a hole in the spectrometer yoke, a $3\frac{1}{2}$-in. liquid hydrogen target, a second sweeping magnet, and finally was monitored by a pressurized hydrogen ion chamber preceded by 6.5 inches of copper. Momentum analysis of the pions was by a double-focusing zero-dispersion spectrometer[10] set for

$\Delta p/p = 1\%$. Pions were counted in a single 10-in. Čerenkov counter filled with paraffin oil. The spectrometer field removed low-energy particles coming from the collimator, and the second sweeping magnet reduced the empty-target background by a factor of 2-3, because pions produced in the copper could not enter the spectrometer. At 135° the same arrangement was used, but the photons did not pass through the spectrometer and the second sweeping magnet was absent. On the basis of pulse-height distributions taken simultaneously with most data points, counter efficiency is estimated to be greater than 90%. The efficiency for the 180°, 500-Mev point may be somewhat less. The pulse height varied with pion momentum but was always well separated from the majority of background pulses. Pion pairs could possibly have contributed to the 500-Mev, 180° point; but the reversed-field count showed this effect to be quite small.

A correction was made for decay in flight without allowing for the possible detection of the resultant muons. This correction varied from 45% to 37% over the range of pion momenta. The effect of a more accurate treatment of the decay was estimated to be 10% or less insensitive to spectrometer settings.

Empty-target data were taken for most of the points reported, and linear interpolation used for some intermediate photon energies. At 180° the empty-target rate was 20-33% of the full-target rate, and at 135° it was 2.5-10%. Except for statistical variations, the empty-target counts decreased smoothly with increasing spectrometer momentum settings.

It is estimated that the absolute accuracy of these points is about 25%, with the relative comparison between 135° and 180° valid to 10% plus statistical error. The thick-target γ-ray spectrum used was computed by R. Alvarez. Saturation of the ion chamber appeared at much higher current levels than those occurring during data-taking. Absolute normalization was effected by use of elastic scattering of electrons in liquid hydrogen and integration over primary electron energies.[11] The 135° resolution curve measured gave good agreement with that calculated for Fig. 1. The recoil momentum of the scattered electrons was equal to that of π^+ mesons at 135° from 700-Mev γ rays. The cross section for electron scattering was taken to be 2.18×10^{-33} cm^2/sr at 600 Mev and 135°, with small corrections for energy loss due to ionization and radiation losses.[12] A correction of 12% for the change in effective target length at 180°, relative to 135°, was applied to the 180° data; this number was taken from previously measured profiles of this spectrometer. The absolute energy calibration is accurate to better than 1% in photon energy as measured by the position of the electron elastic-scattering peak. The spectrometer field was measured with a rotating coil, and the current in the magnets was measured with a precision shunt. These gave agreement of 1 part in 1000 at each momentum setting over a period of two days. The correction for the pion energy loss in the liquid H_2 shifts the 135° and 180° peaks upward by ~9 Mev. χ^2 and F tests give no evidence for other than statistical variations between runs.

We draw the following conclusions:

(a) At 180° there is strong evidence for a peak at a photon energy of 700 ± 7 Mev (corrected for ionization energy loss in the target).

(b) The width of the peak observed at 180° could be instrumental.

(c) At 135° the peak is larger and broader than at 180°; the width is approximately 50 Mev. It appears shifted upwards, relative to the 180° data, by 10 Mev.

The narrowness of the peak at 180° gives further support to the explanation that it is the effect of a single resonant state. The shift observed at other angles could be explained by the energy dependence of terms interfering with the non-spin-flip part of the resonant amplitude. However, it appears very difficult to explain the peak observed in the π^--p total cross section in terms of the same resonant state. In effect, it is hard to explain a shift in the position of the peak by an amount significantly larger than the width of the resonance. It is an open question as to what mechanism could lead to so narrow a resonance.

The authors express their thanks to Professor W. K. H. Panofsky for continual encouragement and discussions. They also benefitted greatly from frequent discussions with Professor B. Richter, and are greatly indebted to E. A. Allton who constructed the liquid hydrogen target. The expert and skillful cooperation of Lynn Boyer in setting up the experiment and of the accelerator crew in maintaining a high-energy electron beam are appreciated.

*This work was supported by the joint program of the Office of Naval Research, the U. S. Atomic Energy Commission, and the Air Force Office of Scientific Research.

[1]H. C. Burrowes, D. O. Caldwell, D. H. Frisch,

D. A. Hill, D. M. Ritson, R. A. Schluter, and M. A. Wahlig, Phys. Rev. Letters 2, 119 (1959).

[2]J. C. Brisson, J. F. Detoeuf, P. Falk-Vairant, L. van Rossum, G. Valladas, and L. C. L. Yuan, Phys. Rev. Letters 3, 561 (1959); also, J. C. Brisson, J. F. Detoeuf, P. Falk-Vairant, L. van Rossum, and G. Valladas, Nuovo cimento (to be published).

[3]T. J. Devlin, B. C. Barish, W. N. Hess, V. Perez-Mendez, and J. Solomon, Phys. Rev. Letters 4, 242 (1960).

[4]M. Heinberg, W. M. McClelland, F. Turkot, W. M. Woodward, R. R. Wilson, and D. M. Zipoy, Phys. Rev. 110, 1211 (1958).

[5]F. P. Dixon and R. L. Walker, Phys. Rev. Letters 1, 142 (1958); 1, 458 (1958). Also, F. P. Dixon, Ph. D. thesis, California Institute of Technology, 1959 (unpublished).

[6]M. Beneventano, G. Finocchiaro, R. Finzi, L. Mezzetti, L. Paoluzzi, and C. Schaerf, Nuovo cimento 17, 274 (1960).

[7]In what follows, the "width" of the peak is to be understood as the full width at half-maximum.

[8]R. L. Walker, in Proceedings of the 1960 Annual International Conference on High-Energy Physics at Rochester (Interscience Publishers, Inc., New York, 1960), p. 17.

[9]M. J. Moravcsik, Phys. Rev. 104, 1451 (1956).

[10]R. A. Alvarez, K. L. Brown, W. K. H. Panofsky, and C. T. Rockhold, Rev. Sci. Instr. 31, 556 (1960).

[11]W. K. H. Panofsky and E. A. Allton, Phys. Rev. 110, 1155 (1958).

[12]F. Bumiller (private communication).

ELASTIC AND QUASI-ELASTIC COLLISIONS OF PROTONS WITH MOMENTA BETWEEN 9 AND 25 Gev/c

G. Cocconi, A. N. Diddens, E. Lillethun, and A. M. Wetherell
CERN, Geneva, Switzerland
(Received February 3, 1961)

The analysis of the interactions of ultrarelativistic[1] cosmic-ray nucleons has provided some evidence that these particles often emerge from collisions against nucleons at rest with little loss of energy (quasi-elastic collisions). It has appeared difficult to reconcile this behavior with the Fermi statistical model, which was the most commonly accepted description of the ultrarelativistic nucleon-nucleon interaction. Recently, however, theoretical arguments have been advanced[2,3] for expecting quasi-elastic collisions.

The CERN 25-Gev proton synchrotron is an intense source of monochromatic ultrarelativistic protons with which phenomena of this kind can now be quantitatively studied. This Letter describes the results of a first series of experiments in which quasi-elastic collisions have actually been observed.

The proton beam utilized was the internal circulating beam. These protons are well collimated and of well-defined energy. Their energy spread is due partly to the ionization losses experienced in the multiple traversals of the target (~100 Mev) and partly to the fluctuations of the top energy from burst to burst, also of the same order of magnitude. The internal target was a Be foil 50 μ thick and the region of the target hit by the protons was roughly circular, about 1 cm in diameter.[4] The protons, scattered by the target at an angle $\theta = 60$ mrad, first passed through an iron collimator, 6 mm wide, 3 cm high, and 1.5 m long, placed 30 m away[5]; the collimated proton beam was then momentum-analyzed by a 4-m long bending magnet (bending angle 90 mrad) and detected by a double coincidence telescope consisting of two scintillators each 1 cm wide and 2 cm high, placed 25 m away from the magnet. The resolving power $\Delta p/p$ of this arrangement was about 1% and was determined by source dimension, slit width, counter width, scattering in the air, energy spread of the circulating beam, and the Fermi motion of the nucleons in the target.

Figure 1 shows the momentum spectra observed for nine values of the circulating beam momentum. The scales given for the cross sections were deduced from another scattering measurement, performed with the external proton beam. Their absolute values must be considered only indicative, as an error even larger than two cannot be excluded at this time.

In the first seven spectra of Fig. 1, two peaks are well resolved. We call the most energetic one the elastic peak, and the second one the quasi-elastic peak. In all nine spectra a continuum is also present, the quasi-elastic continuum, extending from the largest momenta to the lowest. Eventually, this continuum merges with that due to the already well-known process of multiple production.

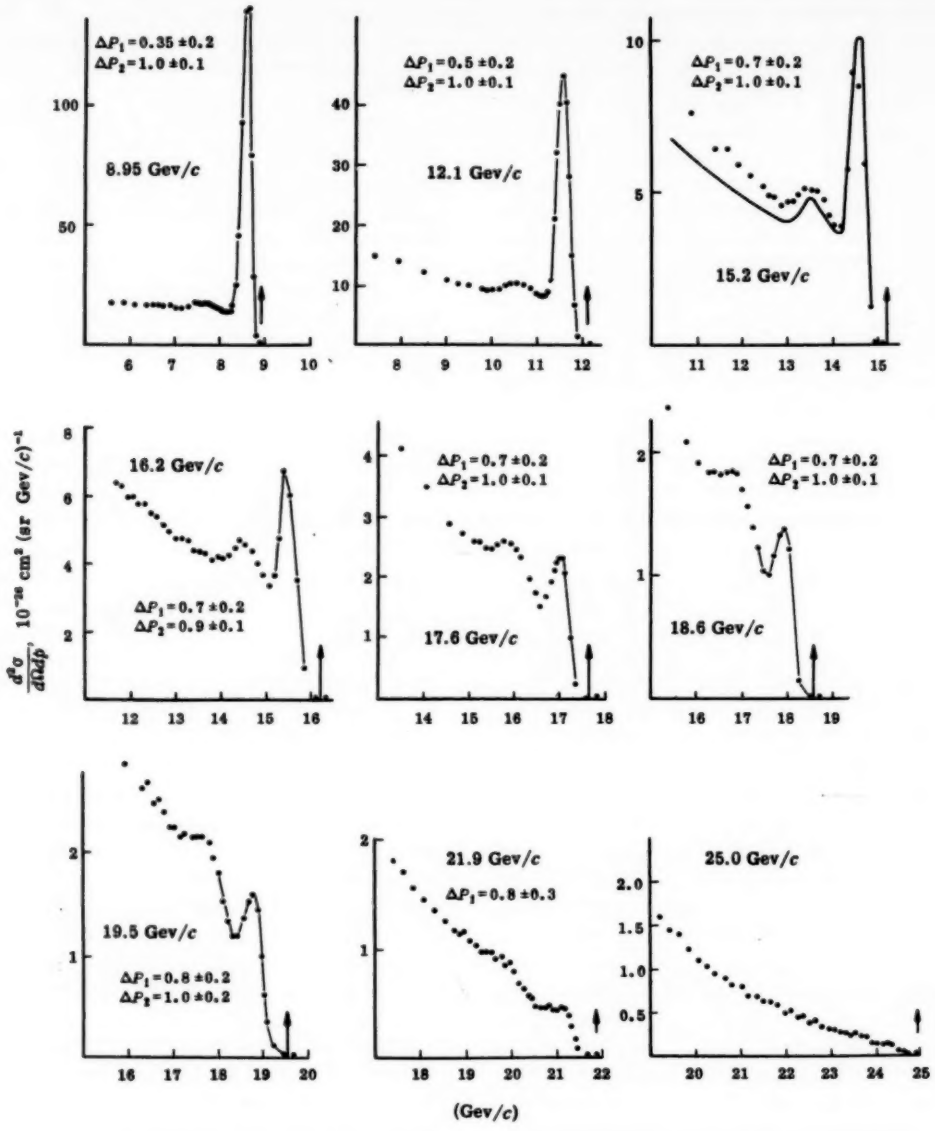
$\Delta P_1 = 0.35 \pm 0.2$
$\Delta P_2 = 1.0 \pm 0.1$
8.95 Gev/c
$\Delta P_1 = 0.5 \pm 0.2$
$\Delta P_2 = 1.0 \pm 0.1$
12.1 Gev/c
$\Delta P_1 = 0.7 \pm 0.2$
$\Delta P_2 = 1.0 \pm 0.1$
15.2 Gev/c
16.2 Gev/c
$\Delta P_1 = 0.7 \pm 0.2$
$\Delta P_2 = 0.9 \pm 0.1$
$\Delta P_1 = 0.7 \pm 0.2$
$\Delta P_2 = 1.0 \pm 0.1$
17.6 Gev/c
$\Delta P_1 = 0.7 \pm 0.2$
$\Delta P_2 = 1.0 \pm 0.1$
18.6 Gev/c
19.5 Gev/c
$\Delta P_1 = 0.8 \pm 0.2$
$\Delta P_2 = 1.0 \pm 0.2$
21.9 Gev/c
$\Delta P_1 = 0.8 \pm 0.3$
25.0 Gev/c
$\frac{d^2\sigma}{d\Omega dp}$, 10^{-28} cm^2 (sr Gev/c)$^{-1}$
(Gev/c)

FIG. 1. Momentum spectra of the positive particles emitted at 60 mrad to the internal proton beam by a Be target. For each spectrum are given, in Gev/c, the momentum of the circulating beam (arrow), Δp_1 = momentum of circulating beam - momentum of elastic peak, Δp_2 = momentum of elastic peak - momentum of quasi-elastic peak. At 15.2 Gev/c, the line corresponds to the spectrum observed with a tantalum target, roughly normalized to that observed with the Be target. The cross sections are "per nucleon" of the Be nucleus.

We believe that the particles detected in the elastic peak, the quasi-elastic peak, and the quasi-elastic continuum are protons and that they are produced in the interaction of the primary protons with the single nucleons of the Be nuclei. Mesons can be excluded on the ground that, at 25-Gev operating energy and $\theta = 110$ mrad, the ratio mesons/protons decreases steadily for increasing energy of the secondaries and is already 1/30 at 18 Gev.[6] We have also found in another measurement at 25-Gev operating energy and for angles $\theta \leq 50$ mrad that the negative secondaries

with momenta above 20 Gev/c are negligible in comparison with the positive ones. Hyperons can be ruled out because the particles we observed must have lifetimes, at rest, greater than $\sim 10^{-8}$ sec.

In order to be convinced that the quasi-elastic protons were produced in proton-nucleon collisions, a run was made, at 15.2 Gev/c, with a tantalum ($A = 181$) target. It gave exactly the same features as the Be run (see Fig. 1), thus showing, within the accuracy of the measurement, that the phenomena here discussed were not influenced by the atomic number of the target.

The elastic peak is then interpreted as due to the diffraction scattering of the protons by the nucleons. This is confirmed by the fact that experimentally the difference between the momentum of the circulating beam and that of the elastic peak, Δp_1, satisfies, within the experimental errors, the relation $\Delta p_1/mc = \frac{1}{2}\gamma^2\theta^2$ ($\gamma >> 1$, $\theta << 1$) which expresses the momentum loss due to the elastic nucleon recoil. If the Fermi motion of the nucleons in the nuclei is taken into account, the disappearance of the elastic peak at 60 mrad for momenta around 20 Gev indicates a characteristic radius of interaction of about 1 fermi.

The quasi-elastic continuum could be interpreted as the result of the exchange of a virtual neutral pion as described by Salzman and Salzman[2] and by Drell.[3] The cross sections evaluated by Drell are in fair agreement with those observed. The quasi-elastic continuum is present at all momenta, thus indicating an angular distribution wider than that of the elastic scattering, also as predicted by Drell. It is worth pointing out that the cross sections for positive secondaries predicted by the statistical model, as evaluated by Hagedorn,[7] are about a factor of 10^3 smaller than those observed at 4 Gev/c below the elastic peak and even smaller at the quasi-elastic peak.

The most unexpected result is the discovery of the quasi-elastic peak. The reality of its existence is confirmed by other measurements performed at $\theta = 20$ mrad and at $\theta = 40$ mrad (Fig. 2). The experimental layouts at these two angles were similar to that described for $\theta = 60$ mrad, except that the doughnut walls were in the path of the scattered beams and corresponded to 100 and 50 g cm^{-2} of iron, respectively. Large errors are introduced into the computation of the solid angle and hence in $d\sigma/d\Omega$ as the distortions produced by the fringing fields of the accelerator are strongly momentum dependent at these angles

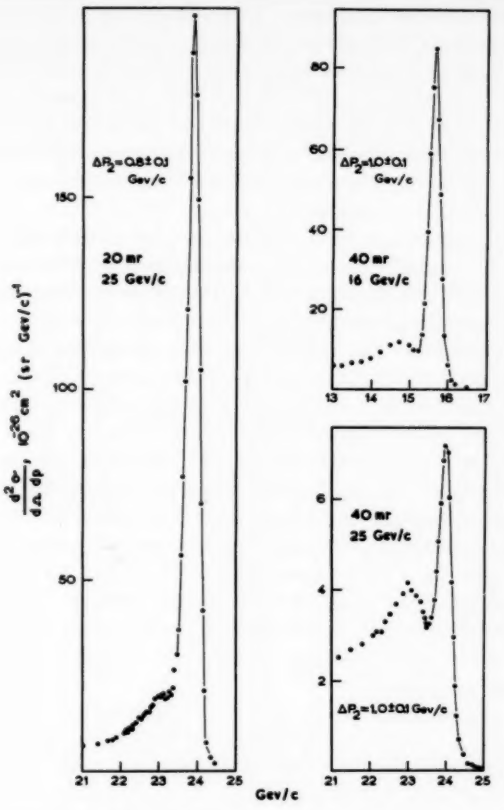

FIG. 2. Momentum spectra at 20 and 40 mrad to the circulating beam, observed with Be targets.

and not yet well evaluated. Nevertheless, from Figs. 1 and 2 it is clear that the quasi-elastic peak is present whenever and only when the elastic peak is present and that the momentum difference between the two peaks, Δp_2, is, within experimental errors, constant and equal to ≈ 1 Gev/c, independent of scattering angle and proton momentum.

The correlation between the quasi-elastic peak and the elastic peak seems to rule out the possibility that the quasi-elastic peak is due to the exchange of a single π^0, enhanced by the well-known resonances observed in the pion-nucleon interaction for pion total energies around $c\Delta p_2$.

Following a suggestion by L. van Hove, the observed features could instead be explained by assuming that the quasi-elastic peak is due to the diffraction disintegration of the target nucleons induced by the ultrarelativistic protons. Repeating for the nucleon-nucleon interaction the arguments discussed by Good and Walker[8] for the

nucleon-nucleus case, it is possible to predict that the diffraction dissociation of the target nucleon into a nucleon and a pion must take place, at our energies, only when ~1 Gev is absorbed and that it must be present, of course, only when the elastic diffraction scattering is present. Only further experiments will enable us to confirm, or not, this suggestive interpretation.

Finally, we want to point out that the existence of the quasi-elastic collisions (the quasi-elastic continuum) for ultrarelativistic protons can have interesting applications.

One concerns radiochemistry. When the quasi-elastic event takes place for the target nucleon embedded in a nucleus it is easily seen that the final momentum of the target nucleon, in the lab system, can be so small as to leave the nucleon inside its original nucleus. The exchange of a pion can then give rise to a nuclear reaction of the type $X_Z{}^A(p,p\pi^{\mp})Y_{Z\pm1}{}^A$. The cross sections evaluated for this phenomenon seem to be of the right order of magnitude for explaining several reactions of this kind, as well as others of similar character, produced by ultrarelativistic protons.[9]

A second remark concerns the possibility of using quasi-elastic events for building a separator of ultrarelativistic antiprotons. Whereas it is expected that the quasi-elastic cross section of antiprotons is equal to that of the protons, the mesons should have quasi-elastic cross sections substantially smaller, being unable to exchange a single pion with a nucleon. A monochromatic secondary beam of ultrarelativistic negative particles containing antiprotons, pions, K mesons, and muons should then, when scattered by a target, give a tertiary beam of quasi-elastic particles enriched in antiprotons according to the ratio of the cross sections. Guesses about intensities and cross sections seem to indicate that such a separator could be of value for bubble chambers at momenta where most of the separators suggested so far will certainly fail. A separator of this kind would also be relatively cheap.

These measurements would have been impossible without the warm collaboration of the proton synchrotron staff. We want to thank in particular Mr. J. Gervaise, who acted as liaison man between our group and the Machine Group. We also thank Mr. C. A. Stahlbrandt for his skillful help with the electronics.

[1]The term ultrarelativistic is used here for a nucleon with Lorentz factor γ = total energy/rest mass >> 1.

[2]F. Salzman and C. Salzman, Phys. Rev. Letters 5, 377 (1960).

[3]S. D. Drell, Phys. Rev. Letters 5, 342 (1960).

[4]K. H. Reich, CERN Internal Report MG-VA 60-37 (unpublished).

[5]The angle of 60 mrad was chosen because, for the time being, it is the smallest angle at which the particles from the target can leave the doughnut through a Mylar window.

[6]G. von Dardel group (private communication).

[7]J. v. Behr and R. Hagedorn, CERN Internal Report 60-20 (unpublished).

[8]M. L. Good and W. D. Walker, Phys. Rev. 120, 1857 (1960) [see also E. L. Feinberg and I. I. Pomeranchuk, Suppl. Nuovo cimento 3, 652 (1956)].

[9]T. I. O. Ericson, F. Selleri, and R. Van de Walle (private communication).

SEARCH FOR THE ω^0 IN PHOTOPRODUCTION

K. Berkelman,* G. Cortellessa, and A. Reale
Laboratori di Fisica, Istituto Superiore di Sanità, Roma, Italy
(Received February 8, 1961)

A recent investigation by Abashian, Booth, and Crowe[1] of the He^3 recoil momentum spectrum in the reaction

$$p+d\rightarrow He^3+\ldots, \tag{1}$$

has revealed, in addition to the peak associated with π^0 production and the continuum associated with double-pion production,

$$p+d\rightarrow He^3+\pi^0, \tag{2}$$

$$p+d\rightarrow He^3+\pi^+ +\pi^-, \tag{3}$$

$$p+d\rightarrow He^3+\pi^0+\pi^0, \tag{3'}$$

an anomalous peak which has been interpreted as being associated with a resonant state of two pions or a particle of mass 310 ± 10 Mev. In the following we shall refer to this particle or resonance (the distinction is perhaps only a matter of lifetime) as if it were a particle ω^0:

$$p+d\rightarrow He^3+\omega^0. \tag{4}$$

In the present experiment we have attempted to produce the ω^0 by the reaction

$$\gamma + p \rightarrow p + \omega^0, \tag{5}$$

using the bremsstrahlung beam of the Frascati 1-Bev electron synchrotron. If the ω^0 is actually a two-pion resonant state, one would expect a rapid breakup into two pions:

$$\omega^0 \rightarrow \pi^+ + \pi^-, \tag{6}$$

$$\omega^0 \rightarrow \pi^0 + \pi^0. \tag{6'}$$

If the ω^0 is instead a new particle, a fast decay into two pions still seems quite likely. An alternate decay mode,

$$\omega^0 \rightarrow \pi^0 + \gamma, \tag{7}$$

if it existed, would probably have been detected by Gomez et al.[2] in their search for the "B^0 meson." An attempt at detecting the ω^0 was then made on the basis of its expected mass and the charged-pion decay mode.

The experimental arrangement is shown in Fig. 1 and is quite similar to that used by Cortellessa and Reale in studying the photoproduction of π^0 mesons.[3] The collimated bremsstrahlung photon beam passed through a liquid hydrogen target and was monitored by the quantameter.[4] The recoil photons were detected by a range telescope (four scintillators in coincidence, one in anticoincidence) with a 20-Mev definition in gamma-ray energy. On the other side the π^+ and π^- from the decay of the ω^0 were detected by two scintillation counters in coincidence placed behind 15 radiation lengths of lead. The lead made the pion telescope less sensitive to neutral pions and gamma rays as well as reducing the singles rates, which would have been quite intolerable since the telescope had a rather large area and was placed at a small angle to the beam. The kinematics conditions fixed by the proton energy and angle were chosen to enable the ω^0 to be produced with enough laboratory energy so that its decay pions would come out in a small cone and could be caught with good efficiency by the pion telescope.

There is no experimentally observable difference between the production of an ω^0 of mass 310 Mev, decaying rapidly into two pions, and the direct production of two pions with a total energy of 310 Mev in their own center-of-mass system:

$$\gamma + p \rightarrow p + \pi^+ + \pi^-. \tag{8}$$

That is, a pair of pions produced with a Q (total kinetic energy in their c.m. system) of 30 Mev will be counted in the pion telescope with exactly the same efficiency as if it had come from the decay of an ω^0. The ω^0 should show up only as a peak in the double-pion Q spectrum at the energy

$$Q = M_{\omega^0} - 2m_{\pi} = 30 \text{ Mev}.$$

By fixing the proton recoil energy and angle and the incident gamma-ray energy, one determines the Q of the pion-pion system. Then, varying the incident gamma-ray energy, one traces out the Q spectrum for the double-pion production, provided that the production cross section does not vary significantly over the range of incident photon energy scanned. Because of the fact that the gamma-ray beam is not monoenergetic but instead has the well-known bremsstrahlung spectrum, one obtains after appropriate normalization the integral Q spectrum for double-pion

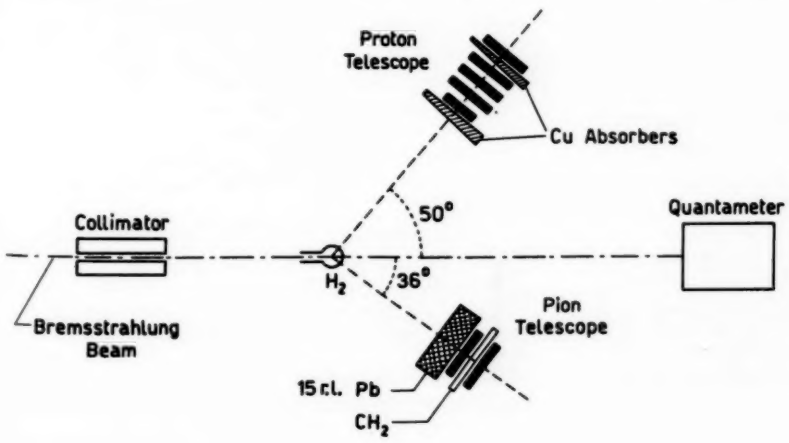

FIG. 1. The experimental setup (not drawn to scale).

production. This integral spectrum should be a smoothly increasing function of Q (reaction 8) with a superimposed step at $Q = M_{\omega^0} - 2m_\pi$ due to ω^0 production and decay (reactions 5 and 6).

In the present experiment the threshold for producing the ω^0 with a recoil proton at an energy of 160 Mev at 50° in the lab system was 950 Mev. The beam energy was varied from 880 Mev (below the double-pion threshold for these conditions) to 1020 Mev, thus scanning Q from zero to 65 Mev, or M_{ω^0} from 280 to 345 Mev. Starting from a background rate of about 0.05 count/10^{10} equivalent quanta, probably due to neutral pion decays, the counting rate (Fig. 2) shows a fairly smooth rise with energy, presumably due to pion-pair production, with no statistically significant ω^0 threshold step. The errors shown represent only counting statistics. Any systematic errors are not expected to vary significantly with energy or affect the interpretation of the data. Also plotted in Fig. 2 is the expected counting rate calculated under the following assumptions: (1) The pion-pion Q spectrum is proportional to phase space, (2) the laboratory differential cross section $d\sigma/d\Omega_p$ for double-pion production with proton recoil at the angle and energy selected in the experiment is

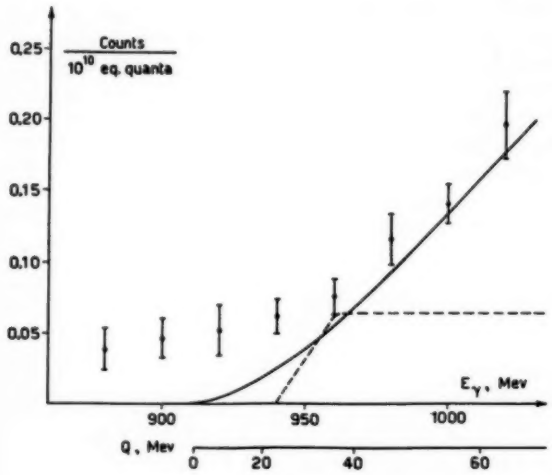

FIG. 2. The counting rate, corrected for pion telescope efficiency, as a function of the bremsstrahlung end-point energy. The corresponding Q of the $\pi\pi$ system (reaction 8) is shown by the bottom scale. The solid curve shows the expected yield from reaction 8; the dashed curve shows the yield from reaction 5 assuming $d\sigma/d\Omega = 0.1$ μb/sr.

about 5 μb/sr,[5] and (3) there is no ω^0. The dashed curve shows the ω^0 contribution for an assumed 0.1-μb/sr production cross section. From Fig. 2 one can set an upper limit for the center-of-mass differential cross section for reaction 5:

$$d\sigma/d\Omega < 0.05 \ \mu\text{b/sr},$$

at $E_\gamma \approx 950$ Mev and $\theta_{\text{c.m.}} = 63°$. This limit holds for any ω^0 mass between 280 Mev and 330 Mev. It should be noted that the ω^0 peak observed by Abashian et al. is about 1/5 as large as their π^0 peak and is easily observed superimposed on the double-pion spectrum. The ω^0 photoproduction yield in the present experiment is less than 1/30 of the π^0 yield at the same energy and angle and is certainly small compared with the direct double-pion yield.

It seems reasonable that if the ω^0 were a resonant state of two pions causing an anomalous final-state interaction in double-pion production, it should show up about as strongly relative to normal double-pion production in the $\gamma + p$ process as it did in the $p + d$ process. This is clearly not the case. There are at least two other alternatives. (1) The ω^0 could be a particle which somehow has an anomalously small photoproduction cross section. (2) The ω^0 could be a long-lived particle or give decay products not detectable in the pion telescope. Even in the latter case one can set an upper limit on the photoproduction cross section using the proton recoil data alone, in the manner of Bernardini et al.[6] The present experiment gives the same upper limit as reference 6:

$$d\sigma/d\Omega < 0.3 \ \mu\text{b/sr}.$$

---

*On leave from Cornell University, visiting scientist at the Istituto Superiore di Sanità with a grant from the National Science Foundation.

[1]A. Abashian, N. E. Booth, and K. M. Crowe, Phys. Rev. Letters 5, 258 (1960).

[2]R. Gomez, H. Burkhardt, M. Daybell, H. Ruderman, M. Sands, and R. Talman, Phys. Rev. Letters 5, 170 (1960).

[3]G. Cortellessa and A. Reale, Nuovo cimento 18, 1265 (1960).

[4]R. R. Wilson, Nuclear Instr. 1, 101 (1957).

[5]B. M. Chasan, G. Cocconi, V. T. Cocconi, R. M. Schectman, and D. H. White, Phys. Rev. 119, 811 (1960).

[6]C. Bernardini, R. Querzoli, G. Salvini, A. Silverman, and G. Stoppini, Nuovo cimento 14, 268 (1959).

PION-PION INTERACTION AND HIGH-ENERGY $p+d$ COLLISIONS

J. G. Taylor*
Laboratoire de Physique Théorique et Hautes Energies, Faculté des Sciences, Orsay, France
and the Institut des Hautes Etudes Scientifiques, Paris, France
(Received February 10, 1961)

A possible explanation of the anomaly found in meson production in proton-deuteron collisions[1] has recently been put forward by Tubis and Uretsky.[2] They suggest that if a final state P-wave pion-pion interaction, described in the scattering length approximation, is added to the statistical model of Abashian et al.,[1] a P-wave scattering length of magnitude 2.5 pion Compton wavelengths explains the anomaly. We wish to present evidence here that does not agree with such a large value for this scattering length. This evidence comes from equations relating the three scattering lengths as derived from crossing symmetry, and from the experimental evidence on the asymmetry of the pion momentum spectrum in τ decay.

We will use the crossing symmetry equations[3] for pion-pion scattering,

$$\tfrac{1}{3}(A_0 - A_2)(\nu, \cos\theta) = \tfrac{1}{2}(A_1 + A_2)(\nu_C, \cos\theta_C), \quad (1)$$

where A_I is the pion-pion scattering amplitude with isotopic spin I, ν is the squared momentum in units of the pion mass, and θ the scattering angle, both in the center-of-mass system, while ν_C, θ_C are the crossed variables $\nu_C = \frac{1}{2}\nu(1+\cos\theta) - (\nu+1)$, $\nu_C \cos\theta_C = \frac{1}{2}\nu(1+\cos\theta) + (\nu+1)$. We will approximate $A_I(\nu, \cos\theta)$ by keeping only the S and P waves, which should be a good approximation in the low-energy region. We take ν, ν_C near the symmetry point $-2/3$, and $\cos\theta$, $\cos\theta_C$ near zero. We assume[3] that the partial-wave amplitudes $A_I(\nu)$ are analytic in the cut ν plane with cuts from $-\infty$ to -1 and 0 to ∞, so that with $\nu_C = \nu + x$, Eq. (1) becomes

$$\tfrac{1}{3}(x+\nu)\int [a_0(\nu') - a_2(\nu')](\nu' - \nu)^{-1} d\nu' - \tfrac{1}{2}(x+\nu)\int a_2(\nu')(\nu' - \nu - x)^{-1} d\nu' = \tfrac{3}{2}(x + 3\nu + 2)\int a_1(\nu')(\nu' - \nu - x)^{-1} d\nu'. \quad (2)$$

In Eq. (2) the integrals are along the real axis except for the interval $(-1, 0)$, and the real functions $a_I(\nu)$ are the absorptive parts of the $A_I(\nu)$. Equation (2) is true for x in a small neighborhood of 0 and for ν near $-\frac{2}{3}$, so we may equate coefficients of powers of x in the power series expansion in x on each side of Eq. (2) to obtain

$$\nu\int [\tfrac{1}{3}a_0(\nu') - \tfrac{5}{6}a_2(\nu')](\nu' - \nu)^{-1} d\nu' = \tfrac{3}{2}(2 + 3\nu)\int a_1(\nu')(\nu' - \nu)^{-1} d\nu'. \quad (3)$$

Each side of Eq. (3) is an analytic function of ν in the cut ν plane and these functions are equal in a real interval near $\nu = -2/3$, so they are equal everywhere. In particular

$$\frac{1}{3}a_0(\nu) - \frac{5}{6}a_2(\nu) = \left(\frac{3}{\nu} + \frac{9}{2}\right)a_1(\nu),$$

$$\frac{1}{3}A_0(\nu) - \frac{5}{6}A_2(\nu) = \left(\frac{3}{\nu} + \frac{9}{2}\right)A_1(\nu). \quad (4)$$

In the scattering length approximation $A_I(\nu) = a_I$, $a_I(\nu) = a_I \nu^{1/2} (I = 0, 2)$, $A_1(\nu) = a_1\nu$, $a_1(\nu) = a_1 \nu^{5/2}$, then in the limit of small ν, Eqs. (4) become

$$a_0 - \tfrac{5}{2}a_2 = 9a_1,$$

$$a_0^2 = \tfrac{5}{2}a_2^2. \quad (5)$$

We use also the result of the analysis of the asymmetry of the pion momentum spectrum in τ decay[4,5] that[6]

$$a_2 - a_0 \approx 0.7. \quad (6)$$

This gives two possible solutions to Eqs. (5) and (6):

$$(a_0, a_1, a_2) = (-1.9, +0.1, -1.2) \text{ or } (-0.4, -0.1, +0.3). \quad (7)$$

Both these solutions have $|a_1| \sim 0.1$, which is two orders of magnitude smaller than the value $|a_1| \sim 15$ required by Tubis and Uretsky. In order to obtain this larger value of $|a_1|$ it is necessary to choose $(a_0, a_2) = \pm(-15, 50)$ or $\pm(740, 240)$. For such large values of the scattering lengths the τ-decay analysis leading to Eq. (6) is no longer good, and it may be possible to explain the existing asymmetry in the pion spectrum in terms of such large scattering lengths. However, the low-energy pion-pion scattering cross section then comes to above 600 barns. This is inconsistent with the values of $\lesssim 0.5$ barn found[7] in the extrapolation procedure applied to the reaction $\pi^- + p \to \pi^- + \pi^0 + p$. Such a strong interaction

should certainly have shown itself in the extrapolation procedure. It also should give a very pronounced peaking at low momentum in the nucleon recoil momentum spectrum, which is definitely not present.[8] Thus we conclude that $|a_1| \sim 15$ is inconsistent with present data and the crossing equations (5).

We note that in the approximation of keeping only S and P waves and applying the properties of crossing, analyticity, and unitarity,[3] it may be shown[9] that the inner regions of the $I=0$ and $I=1$ potentials are attractive and that of the $I=2$ is repulsive. The scattering length solutions of Eq. (7) will both give an $I=0$ resonance,[10] the second solution only will give both an $I=1$ and $I=2$ resonances, while the first solution will give neither an $I=1$ or an $I=2$ resonance.

This is in agreement with the further results obtained at Berkeley on p-d collisions,[11] where a very low energy $I=0$ pion-pion resonance seems to be present. If the anomaly[1] in $p+d \rightarrow \mathrm{He}^3+\pi^0+\pi^0$ is interpreted in terms of a resonance, then this will single out the second pion-pion scattering length solution as the correct one. This assignment is also supported by evidence of strong $I=0$ and $I=1$ pion-pion interactions from pion-nucleon scattering[12] and a strong $I=1$ or $I=2$ pion-pion interaction in the final state of the reaction $\pi^- + p \rightarrow \pi^- + \pi^0 + p$.[13,14]

The data of Pickup et al.[14] are not completely in accord with the second solution, since peaking in the Q value of two pions only appears for backward nucleons for $(\pi^-\pi^0)$ and not for forward nucleons for this pair or forward or backward nucleons for $(\pi^-\pi^+)$. The absence of peaking for forward nucleons is to be expected due to the vanishing of the nucleon-pion vertex, but the absence of peaking in $(\pi^-\pi^+)$ for backward nucleons is disturbing, since $I=0$, 1, and 2 resonances should all contribute, if they exist.

The positions of the predicted resonances are known only very approximately at present.[9] For the first scattering length solution the resonance in $I=0$ is at $\nu_R \approx 1.5$, and for the second solution in $I=0$ is at $\nu_R \approx 2.7$ and in $I=2$ is at $\nu_R \approx 5.0$. The $I=1$ resonance position in the latter case cannot be predicted even approximately, since the value of b is not known. The resonance values for the $I=0$ state are not in agreement with the value[11] $\nu_R \approx 0.2$ found at Berkeley, but we hope to obtain better agreement by machine solution of the S- and P-wave pion-pion equations using the second scattering length solution.

The author would like to thank Professor Lévy and Dr. Motchane for the kind hospitality extended to him while part of this work was being carried out.

---

*On leave of absence from Christ's College, Cambridge, England.

[1]A. Abashian, N. E. Booth, and K. M. Crowe, Phys. Rev. Letters 5, 258 (1960).

[2]A. Tubis and J. L. Uretsky, Phys. Rev. Letters 5, 513 (1960).

[3]For a derivation of these equations see G. Chew and S. Mandelstam, Phys. Rev. 119, 467 (1960).

[4]N. N. Khuri and S. B. Treiman, Phys. Rev. 119, 1115 (1960).

[5]R. F. Sawyer and K. C. Wali, Phys. Rev. 119, 1429 (1960).

[6]We use the results of reference 4, since the results of reference 5 were obtained using only a restricted class of solutions to the S-wave pion-pion problem. For a discussion of this see J. G. Taylor, Proceedings of the 1960 Annual International Conference on High-Energy Physics at Rochester (Interscience Publishers, Inc., New York, 1960), p. 353; and to be published.

[7]J. A. Anderson, P. G. Burke, D. D. Carmony, and N. Schmitz, Proceedings of the 1960 Annual International Conference on High-Energy Physics at Rochester (Interscience Publishers, Inc., 1960), p. 58.

[8]E. Pickup, F. Ayer, and E. O. Salant, Proceedings of the 1960 Annual International Conference on High-Energy Physics at Rochester (Interscience Publishers, Inc., 1960), p. 69.

[9]J. G. Taylor (to be published).

[10]This was already remarked upon by J. G. Taylor, Proceedings of the 1960 Annual International Conference on High-Energy Physics at Rochester (Interscience Publishers, Inc., 1960), p. 740.

[11]Private communication from N. E. Booth.

[12]J. Hamilton, Proceedings of the 1960 Annual International Conference on High-Energy Physics at Rochester (Interscience Publishers, Inc., 1960), p. 289.

[13]J. G. Rushbrooke and D. Radojicic, Phys. Rev. Letters 5, 567 (1960).

[14]E. Pickup, F. Ayer, and E. O. Salant, Phys. Rev. Letters 5, 161 (1960).

$\bar{K}$-NUCLEON BOUND-STATE INTERPRETATION OF THE 1385-Mev π-Λ RESONANCE*

R. H. Dalitz†
Lawrence Radiation Laboratory, University of California, Berkeley, California
(Received February 8, 1961)

The possibility of pion-hyperon resonances associated with "bound states" of the $\bar{K}$-nucleon system was pointed out in some detail several years ago.[1] In view of the clear evidence, recently reported,[2] of a π-Λ resonance at 1385 Mev, it may be of interest to present a simple physical model which may clarify the meaning of the description "bound-state resonance" and which allows a simple picture of its production process qualitatively consistent with all the evidence at present available.

We consider wave functions[3] ψ, ϕ representing the $\bar{K}$-N and π-Y channels, respectively (Y denotes Λ, Σ hyperons), and satisfying the boundary conditions

$$(r\psi)_{r=0} = \alpha \frac{d}{dr}(r\psi)\Big|_0 + \beta \frac{d}{dr}(r\phi)\Big|_0, \qquad (1a)$$

$$(r\phi)_{r=0} = \beta^\dagger \frac{d}{dr}(r\psi)\Big|_0 + \gamma \frac{d}{dr}(r\phi)\Big|_0. \qquad (1b)$$

These boundary conditions represent a zero-range approximation to the interactions within and between these channels. Their form is dictated by the linearity and hermiticity of the Schrödinger equation, the latter requiring also that α be real and γ Hermitian. In the $I=1$ channels, both π-Λ and π-Σ systems participate and ϕ is a 1×2 column matrix, β a 2×1 row matrix, and γ a 2×2 square matrix; β and γ are real if time-reversal invariance holds.

For $\bar{K}$-N elastic scattering, the π-Y channels have outgoing waves, so

$$r\phi = (2\omega_Y)^{-1/2} C e^{iqr}. \qquad (2)$$

Substituting this dependence in (1b), we may eliminate ϕ from these boundary conditions, with the result

$$(r\psi)_0 = \{\alpha + i[\beta q(1-i\gamma q)^{-1}\beta^\dagger]\} \frac{d}{dr}(r\psi)\Big|_0 = (a+ib)\frac{d}{dr}(r\psi)\Big|_0 \qquad (3)$$

This is the boundary condition introduced by Jackson et al.[4] for discussion of $\bar{K}$-N scattering.

When the imaginary part b is small—i.e., the cross-channel interaction parameter β is small (we argue below that γ is not large)—we may approximate the wave function of the system by first neglecting β. If α is negative, Eq. (1a) then allows an eigensolution

$$\psi = \frac{1}{(4\pi\mu_K|\alpha|)^{1/2}} \frac{\exp(-r/|\alpha|)}{r}, \qquad (4)$$

representing an $S_{1/2}$ $\bar{K}$-N bound state of mass $M^* \approx M_N + m_K - 1/(2\mu_K\alpha^2)$, where μ_K denotes the $\bar{K}$-N reduced mass. However, this state is linked with the energetically available π-Y channels. From (1b), the wave function ϕ corresponding to the eigensolution ψ of Eq. (4) can be obtained and the rate of outflow in the π-Y channels can then be computed. This outflow leads to a finite lifetime for the $\bar{K}$-N bound state, corresponding to a half-width

$$\tfrac{1}{2}\Gamma = 2\pi C^\dagger(q/\omega_Y)C = \frac{1}{\mu_K|\alpha|^3}\{\beta(1+iq\gamma)^{-1}q(1-i\gamma q)^{-1}\beta^\dagger\}. \qquad (5)$$

From (3), this bracket is equal to the imaginary part b of the $\bar{K}$-N scattering length, and we have the simple result,[5]

$$\tfrac{1}{2}\Gamma = b/(\mu_K|\alpha|^3). \qquad (6)$$

As is physically reasonable, this width will be small if b is small (i.e., the reaction $\bar{K}+N \to Y+\pi$ has a low rate) or if $|\alpha|$ is large (corresponding to a diffuse structure for the $\bar{K}$-N bound state).

The set of $\bar{K}$-N scattering parameters which corresponds to the possibility of an $I=1$ bound state is the (a -) set of Dalitz and Tuan,[6] for which b_1 is small and a_1 is large and negative. The present K^--p data at low energies lead to $a_1 + ib_1 = -1.08(\pm 0.2) + i0.20(\pm 0.06)$ fermi.[7] With neglect of the energy dependence of these parameters,[8] we then have for the $\bar{K}$-N bound-state parameters (with $\alpha \approx a$, neglecting γ),

$$E_\gamma = M_N + m_K - (2\mu_K a^2)^{-1} = 1382(\pm 20)\ \text{Mev}, \qquad \tfrac{1}{2}\Gamma = b/(\mu_K|a|^3) \approx 18\ \text{Mev}. \qquad (7)$$

The radius parameter of the $\bar{K}$-N state (to be compared with 4.3 fermis for the deuteron) is then $|a| = 1.08$ fermis, so that it is indeed quite diffuse.

To discuss the shape of the π-Λ resonance and the Σ/Λ ratio at resonance, we return to Eqs. (1a) and (1b). For $E < M_N + m_K$, we have

$$r\psi = F(2\mu_K)^{-1/2} e^{-\kappa r}, \tag{8}$$

where $\kappa = [2\mu_K(M_N + m_K - E)]^{1/2}$. Just as we previously eliminated ϕ, ψ can now be eliminated from the boundary conditions, leading to the boundary condition for ϕ,

$$(r\phi)_0 = \Gamma \frac{d}{dr}(r\phi)\Big|_0 = \left(\gamma - \frac{\kappa(\beta^\dagger\beta)}{1+\kappa\alpha}\right) \frac{d}{dr}(r\phi)\Big|_0. \tag{9}$$

We note that, at the resonance energy, the coefficient Γ becomes infinite, as is physically appropriate. The first term of Γ represents "potential scattering"; if γ were large, the resonance would have an asymmetrical form of the type well known in neutron-nucleus resonance scattering.[9] Since this effect is not apparent in the data, we believe that γ is not large (as appears very reasonable for a pion-hyperon state with $j = \frac{1}{2}$), and we will neglect it here compared with the resonance term. The pion-hyperon scattering phases may be obtained by diagonalizing $\Gamma' = q^{1/2}\Gamma q^{1/2}$, with the result

$$\tan\delta_r = -\frac{\kappa(\beta_\Sigma{}^2 q_\Sigma + \beta_\Lambda{}^2 q_\Lambda)}{1+\kappa\alpha}, \quad \tan\delta_{nr} = 0, \tag{10}$$

where δ_r, δ_{nr} denote the resonant and nonresonant phase shifts, respectively. The resonant state has the form

$$|\pi Y, \text{resonant}\rangle = (\beta_\Lambda q_\Lambda{}^{1/2} |\Lambda\pi\rangle + \beta_\Sigma q_\Sigma{}^{1/2} |\Sigma\pi\rangle), \tag{11}$$

and the total π-Λ cross section is

$$\sigma_{\text{tot}}(\pi\Lambda) = \frac{4\pi}{q_\Lambda{}^2} \frac{(\kappa b_\Lambda)^2}{(1+\kappa a)^2 + (\kappa b)^2}, \tag{12}$$

where

$$b = b_\Sigma + b_\Lambda = \beta_\Sigma{}^2 q_\Sigma + \beta_\Lambda{}^2 q_\Lambda$$

is generally energy dependent.

Experimentally,[2] the Σ/Λ ratio at resonance is believed to be less than 10%. From (11), this ratio is given by $R_r = (\beta_\Sigma/\beta_\Lambda)_r{}^2 (q_\Sigma/q_\Lambda)_r$. In the present model, an estimate of this ratio depends on a normalization in terms of the Σ/Λ ratio, $R_t = (\beta_\Sigma/\beta_\Lambda)_t{}^2 (q_\Sigma/q_\Lambda)_t$, for the $I = 1$ channels at the $\bar{K}$-N threshold. The measured value[10] is $R_t = 1.0 \pm 0.8$; a lower limit, $R_t > 0.30 \pm 0.06$, may be obtained from the Σ^-/Σ^+ ratio and the Λ-π^0 rate in K^--p capture at rest. If l_Σ, l_Λ denote the orbital angular momenta in the π-Σ and π-Λ channels, the resonance ratio will be

$$R_t (q_\Sigma/q_{\Sigma t})^{2l_\Sigma + 1} / (q_\Lambda/q_{\Lambda t})^{2l_\Lambda + 1}$$

if the energy dependence of β_Σ, β_Λ is controlled by the centrifugal barriers, that is, $0.8 R_t$ with odd parities for K-Σ and K-Λ, $0.5 R_t$ with even parities for both. We see that it is difficult to obtain a ratio as small as that observed unless the amplitudes β_Σ and β_Λ have some energy dependence beyond that due to the centrifugal barrier effect.

With the $\bar{K}$-N bound-state interpretation, the production of the π-Λ resonant state,

$$\bar{K} + N \to (\bar{K}N) + \pi, \quad (\bar{K}N) \to \Lambda + \pi, \tag{13}$$

is closely analogous with the well-known process of deuteron formation in nucleon-nucleon collisions,

$$N + N \to (NN) + \pi. \tag{14}$$

We note that, for the K^- energies of interest, the pion produced in Reaction (13) travels a distance of approximately 6 fermis in one mean lifetime of the $(\bar{K}N)$ bound state. For the same reason that p-wave pion production is dominant[11] in Reaction (14) above final c.m. momenta ≈ 50 Mev/c, we expect[12] that p-wave pion production will be strong in Reaction (13). This appears consistent with the excitation curve observed.

Further, Reaction (14) is known to take place predominantly in those states where the π-N (3, 3) resonant interaction can be effective. It is reasonable to expect similarly for Reaction (13) that the (3, 3) resonance will play an important role in determining the dominant production states. With this assumption, Y^* production must take place mainly from $I = 1$ initial $\bar{K}$-N states, and we then have the following:

(a) $Y^{*+}/Y^{*-} \approx 1$ for the K^--p reaction, as is consistent with observation except perhaps at the highest energy [for 1150-Mev/c K^- mesons, an energy which is somewhat beyond the (3, 3) resonance region]; and

(b) since $I = 1$ holds for the K^--n and $\bar{K}^0$-p sys-

tems,

$$\sigma(K^- + n \to \pi^0 + Y^{*-})[= 2\sigma(K_2{}^0 + p \to \pi^0 + Y^{*+}]$$
$$= \sigma(K^- + p \to \pi^- + Y^{*+}) + \sigma(K^- + p \to \pi^+ + Y^{*-}). \quad (15)$$

Further,

(c) characteristic correlations then predicted for the (E_+, E_-) plot of the $\Lambda + \pi^+ + \pi^-$ events appear to be qualitatively consistent with the observations.[13]

Also, as for the π^+-d system, the (3, 3) resonance will lead,[14] on the present model, to a rather broad "resonance" in the π-Y^* system for total energy ≈ 1650 Mev.

In conclusion, we remark that the evidence in support of global symmetry from the study of hyperon-nucleon interactions is now quite strong.[15] As Amati et al. have emphasized recently, the occurrence of an $I=1$, $j=\frac{3}{2}$ π-Λ resonance is then to be expected.[16] The predictions of its location (1375 Mev), its half-width (approximately 27 Mev), and its Σ/Λ ratio are all compatible with the Y^* observations. However, despite the remarkable agreement on these points, it must be remembered that the influence of the nearby $\bar{K}$-N channel on the location of this $j=\frac{3}{2}$ resonance may be considerable, and that this resonance may well be displaced to some higher energy value.

Helpful discussions of the experimental data with Dr. Donald H. Miller, Dr. Arthur H. Rosenfeld, and other members of the Hydrogen Bubble Chamber Group at Berkeley are acknowledged with gratitude.

---

*Work done under the auspices of the U. S. Atomic Energy Commission.

†Permanent address: Enrico Fermi Institute for Nuclear Studies, University of Chicago, Chicago, Illinois.

[1]R. H. Dalitz and S. F. Tuan, Phys. Rev. Letters 2, 425 (1959); Ann. Phys. 10, 307 (1960). The possibility of interpreting the observed π-Λ resonance in this way has been discussed recently by M. Ross and G. Shaw, Phys. Rev. Letters 5, 579 (1960).

[2]M. H. Alston, L. W. Alvarez, P. Eberhard, M. L. Good, W. Graziano, H. K. Ticho, and S. G. Wojcicki, Phys. Rev. Letters 5, 520 (1960); M. Ferro-Luzzi, Revs. Modern Phys. (to be published); R. Adair, Revs. Modern Phys. (to be published); O. Dahl, N. Horwitz, D. H. Miller, J. J. Murray, and P. G. White, Phys. Rev. Letters 6, 142 (1961).

[3]For convenience in the later expressions, we normalize each wave function to $(2\omega)^{-1}$, where $\omega = \omega_1\omega_2/(\omega_1+\omega_2)$ is the "reduced energy" in the corresponding two-particle channel.

[4]J. D. Jackson, D. G. Ravenhall, and H. W. Wyld, Nuovo cimento 9, 834 (1958).

[5]This formula is essentially equivalent to that for the lifetime width of the K^--p Coulomb 1s state, after b is replaced by $\frac{1}{2}(b_0+b_1)$ and α by the appropriate Bohr radius. However, the difference in shape between (4) and the Coulomb wave function gives rise to an additional factor of 2.

[6]R. H. Dalitz and S. F. Tuan, Ann. Phys. 8, 100 (1959).

[7]For a discussion of their derivation, see R. H. Dalitz, Revs. Modern Phys. (to be published), Appendix A.

[8]We are anxious to emphasize explicitly that there is little physical reason to expect these parameters a, b to be energy independent. On the contrary, as we note later, a decrease in b with decreasing energy may be expected from phase-space and centrifugal-barrier considerations. However, we have at present no clear guidance concerning what energy dependence to assume, since this will depend on the adoption of a specific model. Ross and Shaw (reference 1) have assumed an effective-range expansion, but the present data are consistent with zero effective range.

[9]See, for example, J. M. Blatt and V. F. Weisskopf, Theoretical Nuclear Physics (John Wiley & Sons, New York, 1952), pp. 401 and 468-9. We note that a small value of γ has quite a strong effect on the shape, and especially on the symmetry, of this resonance, but that it has little effect on its location or width.

[10]L. Alvarez, Lawrence Radiation Laboratory Report UCRL-9354, 1960 (unpublished).

[11]See, for example, M. Gell-Mann and K. M. Watson, Annual Review of Nuclear Science (Annual Reviews, Inc., Palo Alto, California, 1954), Vol. 4, p. 219.

[12]Note that the $\bar{K}$ meson cannot emit a single pion, although it can scatter pions emitted from the nucleon. This can give rise to some s-wave production. Such scattering appears essential if (3,3) π-N resonant enhancement is to occur.

[13]As shown by calculations at present being carried out jointly with D. H. Miller and which will be reported at a later time.

[14]We note that, in the $\pi + (\bar{K}N)$ state with $I=1$, $m_I=0$, the π-N (3,3) resonance has a weighting factor only one-half of that in the π-d state. As a result, the "resonance" effect is not expected to be as marked as is observed in the latter case. Further, because of the large $\bar{K}$-N binding energy, this resonance hump will be greatly broadened relative to the (3,3) resonance, especially on the high-energy side.

[15]R. H. Dalitz, Revs. Modern Phys. (to be published).

[16]D. Amati, B. Vitale, and A. Stanghellini, Phys. Rev. Letters 5, 524 (1960).

ABSTRACTS

In this section are printed the abstracts of Articles that have been forwarded to The American Institute of Physics for publication in THE PHYSICAL REVIEW. In quoting information obtained from this section before the appearance of the corresponding Article, reference should be made to "Physical Review (to be published)" rather than to this Journal.

INCOHERENT MICROWAVE RADIATION FROM A PLASMA IN A MAGNETIC FIELD. Jay L. Hirshfield and Sanborn C. Brown, Department of Physics and Research Laboratory of Electronics, Massachusetts Institute of Technology, Cambridge, Massachusetts (Received December 23, 1960).

The microwave emission from a plasma in a magnetic field is calculated theoretically, using Kirchhoff's radiation law, for cases when characteristic waves do not couple within the plasma. Experimental observations of radiation temperatures and cyclotron radiation line breadth and shape are cited to illustrate applications of the theory to experiment.

SOLID He^4. Louis Goldstein, University of California, Los Alamos Scientific Laboratory, Los Alamos, New Mexico (Received December 30, 1960).

Using a phenomenological approach, it is shown first that solid He^4 in equilibrium with liquid He^4II along the phase separation line, as well as at pressures somewhat above the melting pressure, should have anomalous thermal properties over a finite temperature range or, at least, at isolated temperatures. Such a behavior of the solid results from a correlation of thermodynamic character of its thermal properties with those of the anomalous liquid. The predicted anomalies of the solid will then be effectively verified in terms of rigorous thermodynamics and somewhat incomplete data available on liquid and solid He^4 along the melting line over a finite temperature interval. A specific anomaly of the melting pressure consisting in a shallow temperature minimum will be predicted at low temperatures, where both the liquid and solid phases are assumed to exhibit normal static thermal properties. The persistence of the anomalous equilibrium properties of liquid He^4II on solidification will be discussed qualitatively as suggesting a similar origin of these anomalies in both phases, such a situation having been shown previously to exist with respect to the thermal anomalies of liquid and solid He^3.

GROUND STATE OF LIQUID HELIUM (MASS 4). Fa Yueh Wu and Eugene Feenberg, Washington University, St. Louis, Missouri (Received December 22, 1960).

The wave function describing the ground state of a boson system is approximated by the function $\Psi = \prod \exp \frac{1}{2} u(r_{ij})$. The superposition approximation is then used to derive a linear, inhomogeneous integral equation for du/dr in which the only other quantities occurring are the experimentally observed two-particle distribution function $g(r)$ and its first derivative. A numerical solution for He^4 is computed and compared with the explicit approximate solution derived by Abe. Using the computed $u(r)$ and a proper smooth extrapolation of $g(r)$ into the region below the apparent cutoff at $r = 2.34$ A, the kinetic energy of liquid He^4 at absolute zero is estimated at 2.91×10^{-15} ergs/atom.

A functional $J(du/dr)$ is constructed with the property that Abe's integral equation for du/dr is just the Euler equation associated with the problem of finding a u for which J takes on an extreme value. The extreme value of J (actually a maximum) is simply related to the expectation value of the kinetic energy. The variational property is used to determine the best $u(r)$ from a family of trial functions.

The calculated value of the kinetic energy and the measured total energy are used, in conjunction with the virial theorem, to determine the coefficients of a 6-n Lennard-Jones potential. At $n = 12$, the calculation yields a deeper potential well and a slightly wider repulsive region than is calculated from the properties of the gas phase.

STUDY OF THE INTERNAL FIELDS ACTING ON IRON NUCLEI IN IRON GARNETS, USING THE RECOIL-FREE ABSORPTION IN Fe^{57} OF THE 14.4-kev GAMMA RADIATION FROM Fe^{57m}. R. Bauminger, S. G. Cohen, A. Marinov, and S. Ofer, Department of Physics, The Hebrew

University, Jerusalem, Israel (Received December 22, 1960).

The shape of the recoil-free absorption spectrum obtained in iron garnet absorbers has been investigated, using, as a source, a Co^{57} source embedded in stainless steel. The results confirm the existence of two iron sublattices, each showing a Zeeman structure characterized by different parameters. No significant differences have been detected between the Zeeman structure in yttrium iron garnet and dysprosium iron garnet. The values obtained for the effective magnetic field at the Fe^{57} nuclei at room temperature are 3.90×10^5 oe and 4.85×10^5 oe for the *d* and *a* iron lattice sites, respectively. At liquid air temperature the corresponding fields are 4.6×10^5 oe and 5.4×10^5 oe, respectively. The mean value of the chemical shift for the *d* sites relative to stainless steel is about 0.04 $\pm$ 0.005 cm/sec and about 0.06 $\pm$ 0.005 cm/sec for the *a* sites.

TEMPERATURE DEPENDENCE OF ELECTRON-BOMBARDMENT-INDUCED CONDUCTIVITY IN MgO. II. William C. Schieve* and Martin A. Pomerantz, Bartol Research Foundation of the Franklin Institute, Swarthmore, Pennsylvania (Received December 19, 1960).

Previous measurements of the temperature dependence of the electrical conductivity induced in single crystals of MgO by bombardment with 1.3-Mev electrons over the temperature range 290°-600°K have been extended to 100°K. Two crystals from different sources were investigated.

The bombardment-induced current, I_C, varies linearly with primary current, I_p, at 298°K and at 105°K. However, in certain cases measurements of I_C vs applied voltage, V_C, reveal a deviation from Ohmic behavior which is enhanced at low temperature.

The bombardment-induced conductivity exhibits a maximum near 250°K. Both crystals display a temperature dependence at low temperatures which is consistent with the power-law relationship $I_C/I_p = kT^m$, where $m = 3.3$ and 3.8, respectively.

A rising non-Ohmic I_C vs V_C characteristic appears to be dependent upon the magnitude of the applied field, the onset occurring at 3×10^4 v/cm. Collision ionization and warm carrier phenomena, rather than surface effects, probably account for the observed results.

It is impossible to ascribe the temperature dependence of the bombardment-induced conductivity solely to the temperature variation of the carrier mobility. The results can be explained in terms of change with temperature of both the lifetime and mobility of the charge carriers. A combination of optical mode (polaron), acoustical mode, and ionized impurity scattering is assumed, in addition to a temperature-dependent capture cross section for the carrier. The theoretical curve fits the experimental data satisfactorily, and gives reasonable values for the parameters.

*Present address: U. S. Naval Radiological Defense Laboratory, San Francisco, California.

LOW-TEMPERATURE LATTICE THERMAL CONDUCTIVITY. Joseph Callaway, Division of Physical Science, University of California, Riverside, California (Received December 13, 1960).

The effect of point imperfections on lattice thermal conductivity is discussed with particular attention to the case in which the temperature is low, but the normal three-phonon scattering is still dominant. The experimental results of Walker and Fairbank on the conductivity of isotopic mixtures of solid helium are analyzed.

ABRUPT-KINK MODEL OF DISLOCATION MOTION. A. D. Brailsford, Scientific Laboratory, Ford Motor Company, Dearborn, Michigan (Received December 29, 1960).

A new model of dislocation motion is presented. The behavior of a dislocation in the presence of an applied stress is described in terms of a redistribution of kinks along its length. In contrast with previous models, in which a kink is envisaged as a smooth step extending over many lattice constants, we suppose a kink to be abrupt. Consequently, kink diffusion is considered to be a thermally activated process. Transport equations are formulated which include the effects of generation, diffusion, and collision of kinks. General results obtained from these equations show that a dislocation does not behave like an extensible string in this model. Particular application to small harmonically-time-dependent stresses leads naturally to a new theory of the

Bordoni anelastic peak. The characteristic relaxation time depends on line length as well as the attempt frequency and activation energy for diffusion. As a result the decrease in the peak height and slight lowering of the peak temperature upon alloying or neutron irradiation are explained. Assuming an exponential distribution of line lengths, the results of the theory are used to evaluate the merit of different published values of the activation energy. Calculated attenuation peaks for different frequencies are shown to account for the experimentally observed large half-widths in pure cold-worked metals. The absence of a peak in well-annealed metals is explained if dislocations are then arranged parallel to the close-packed directions, thereby eliminating the kink density. The process by which cold-working annealed materials can give rise to kinks is discussed. Experiments are suggested which might further test the theory.

EFFECTS OF HYDROSTATIC PRESSURE ON THE PARAMAGNETIC RESONANCE SPECTRA OF SEVERAL IRON-GROUP IONS IN CUBIC CRYSTALS. Walter M. Walsh, Jr.,* Gordon McKay Laboratory, Harvard University, Cambridge, Massachusetts (Received December 29, 1960).

The magnetic resonance spectra of Cr^{3+}, Mn^{2+}, Fe^{3+}, and Ni^{2+} present as substitutional impurities in MgO crystals and powders, and of Mn^{2+} in cubic ZnS have been observed as functions of hydrostatic pressure at room temperature. The results are interpreted assuming the local compressibilities to be equal to those of the pure host lattices.

The measured volume dependence of the orbital contributions to the magnetic moments of the F-state ions, Cr^{3+} and Ni^{2+}, are consistent with a point-charge model within the experimental error. This simple model can only crudely account for the observed magnitudes of the orbital singlet-triplet splittings, however.

The pressure dependences of the cubic field splittings of the S-state ions, Mn^{2+} and Fe^{3+}, are identical in MgO and correspond roughly to a fourth-power law if an ionic potential is assumed. The cubic-field parameter for Mn^{2+} in ZnS varies half as rapidly with volume. These results are consistent with recent calculations of Powell, Gabriel, and Johnston if it is assumed that the volume dependences of the cubic potentials in these lattices are given by the ionic model, though the relative magnitudes are not.

The hyperfine structure of the manganese spectra also proves sensitive to sample volume, particularly in the sulfide. The effect may be qualitatively understood in terms of the exchange-polarization theory of the strong electron-nuclear interaction.

*Now at Bell Telephone Laboratories, Murray Hill, New Jersey.

FERROELECTRICITY IN $Bi_4Ti_3O_{12}$ AND ITS SOLID SOLUTIONS. E. C. Subbarao, Solid State Phenomena Department, Westinghouse Research Laboratories, Pittsburgh, Pennsylvania (Received December 21, 1960).

On the basis of dielectric studies on polycrystalline specimens, $Bi_4Ti_3O_{12}$ has been established as a ferroelectric with a Curie temperature of 675°C. The symmetry is orthorhombic with $a = 5.411$ A, $c = 32.83$ A, and $b/a = 1.007$ at 25°C. A high-temperature x-ray study revealed a symmetry change to tetragonal at 675°C. The polar axis is probably the orthorhombic b axis. $Bi_4Ti_3O_{12}$ is a member of oxides with the general formula $(Bi_2O_2)^{2+}(Me_{X-1}R_XO_{3X+1})^{2-}$. According to Aurivillius, the crystal structure of $Bi_4Ti_3O_{12}$ comprises a stacking of Bi_2O_2 and perovskite-like $Bi_2Ti_3O_{10}$ layers along the pseudo-tetragonal c axis. Multiple ion substitutions of $(Bi^{3+}Ti^{4+})$ in $(Bi_2O_2)^{2+}(Bi_2Ti_3O_{10})^{2-}$ by $(Me^{2+}Nb^{5+})$, where Me^{2+} = Ba, Pb, or Sr, lead to a steep decrease of the Curie temperature.

PHOTOCHEMISTRY OF THE V_1 CENTER. J. D. Kingsley,* Department of Physics, University of Illinois, Urbana, Illinois (Received December 27, 1960).

A series of photochemical experiments on the color centers present in KBr and KCl after exposure to x rays at 80°K is discussed. These experiments are chemical in nature, with the reactions being triggered through exposure to radiation of various wavelengths. It is shown that the only V center which has a large electron capture cross section is the V_K center and the cross section of the V_1 center is very small. It is also shown that the destruction of the V_1 center does not involve the annihilation of an elec-

tron or hole trapped at a crystal imperfection but apparently involves the addition of an interstitial to the F center, yielding as a product the undisturbed lattice. The implications of these observations as they relate to the structure of the V_1 center are discussed.

*Present address: General Electric Research Laboratory, Schenectady, New York.

POLARIZATION OF Co^{57} IN Fe METAL. J. G. Dash,* R. D. Taylor, D. E. Nagle, P. P. Craig, and W. M. Visscher, Los Alamos Scientific Laboratory, University of California, Los Alamos, New Mexico (Received December 16, 1960).

A study has been made of the effect of low temperatures on the resonant emission and absorption of 14.4-kev Mössbauer radiation from Fe^{57} in Fe metal. Analysis of intensity changes in the hyperfine spectrum is made in terms of the Zeeman level splittings of the ground states of Fe^{57} absorbing nuclei and of the ground states of Co^{57} parent nuclei. The theory for the temperature dependence is developed in terms of the properties of the Co^{57} decay and of the subsequent gamma transitions. Experiments were carried out with a source of Co^{57} nuclei in Fe metal at temperatures between 4.5° and 0.85°K. The experimental results, analyzed in terms of the theory, yield a value of the hyperfine magnetic field of 300 ± 20 kilogauss at the Co^{57} nuclei. Comparison of the result with other pertinent experimental values indicates that depolarization of the nuclei by the K-capture decay of Co^{57} is not evident in the present material.

*Present address: University of Washington, Seattle, Washington.

FERROMAGNETIC RELAXATION. I. THEORY OF THE RELAXATION OF THE UNIFORM PRECESSION AND THE DEGENERATE SPECTRUM IN INSULATORS AT LOW TEMPERATURES. M. Sparks, R. Loudon, and C. Kittel, Department of Physics, University of California, Berkeley, California (Received December 27, 1960).

A scheme is proposed for the relaxation processes at low temperatures accompanying excitation of uniform precession spin waves in a ferromagnetic resonance experiment, with particular reference to highly pure yttrium iron garnet. The processes are: (1) scattering of uniform precession spin waves into the degenerate spin-wave modes by polishing imperfections on the sample surface; (2) equalization of the populations of the degenerate spin-wave modes, also by surface imperfections; and (3) relaxation of the degenerate modes by Raman scattering of thermal spin waves through the magnetic dipole interaction. Relaxation times for the three processes are calculated and compared with experimental values, with reasonable agreement.

DECAY OF PHOSPHORESCENCE IN $CaCO_3$, $MgCO_3$, $CaMg(CO_3)_2$, AND $CaSO_4$. W. L. Medlin, Field Research Laboratory, Socony Mobil Oil Company, Dallas, Texas (Received November 7, 1960; revised manuscript received January 9, 1961).

The decay of phosphorescence in $CaCO_3$, $MgCO_3$, $CaMg(CO_3)_2$, and $CaSO_4$ obeys the relation, $I = I_0[b/(b+t)]^m$, where the parameters b and m are functions of the temperature of decay and the fraction of initially filled traps (i.e., the activation time). This result can be derived from the usual model for second-order decay and the results predicted for the behavior of b and m with temperature and excitation time are the same whether it is assumed that the traps and luminescent centers are independent of each other or are due to the same defect or impurity center. It is shown, however, that in both cases the predicted behavior is not in agreement with the experimental results for the crystals studied here.

MAGNETIZATION AND ELECTRICAL RESISTIVITY OF ERBIUM SINGLE CRYSTALS. R. W. Green,* S. Legvold, and F. H. Spedding, Institute for Atomic Research and Department of Physics, Iowa State University, Ames, Iowa (Received December 19, 1960).

The magnetic properties of erbium single crystals (hcp) grown by the Bridgman method have been determined in fields up to 18 kiloersteds with the field applied parallel to and perpendicular to the c axis at 4.2°K and between 20.4°K and 300°K. The c axis was found to be the direction of easy magnetization. A Néel

point was observed at 85°K. The ferromagnetic-antiferromagnetic transition temperature inferred from the magnetic data was 19.6°K. The saturation moment, $\sigma_{\infty 0}$, obtained by extrapolation of the c-axis data, was 8 Bohr magnetons compared to the theoretical 9. Electrical resistivity measurements from 1.3°K to 300°K with the current parallel to the c axis showed a sharp increase in resistivity at 20.4°K, the ferromagnetic-antiferromagnetic transition temperature; a large peak occurred at 53.5°K, and a minimum occurred at the Néel point. The a-axis resistivity curve showed a change in slope at the Néel point and was well behaved elsewhere.

*Now at Morningside College, Sioux City, Iowa.

SCINTILLATION RESPONSE OF ACTIVATED INORGANIC CRYSTALS TO VARIOUS CHARGED PARTICLES. R. B. Murray and A. Meyer, Oak Ridge National Laboratory, Oak Ridge, Tennessee (Received December 5, 1960).

Experimental studies of the response of activated ionic crystals such as NaI(Tl) and CsI(Tl) to heavy charged particles indicate decreasing scintillation efficiency with increasing particle mass, and a nonlinearity in pulse height versus energy for heavier particles. Recent experiments indicate that the scintillation efficiency to electrons, however, is less than that to protons. In an attempt to account for these effects, this paper presents a calculation based on a model of the process of energy transfer from the incoming particle to the activator sites. In this model, the energy carriers are taken to be excitons resulting from recombination of electron-hole pairs in the wake of the particle. The migration of carriers to activator sites is described by a one-velocity diffusion equation in which the density of unoccupied activator sites, N_a, is a function of space and time. The diffusion equation is coupled with a second differential equation describing the time dependence of N_a. The solution to these equations indicates that the depletion of available activator sites by a particle with high dE/dx can account for observed saturation effects. This model further contains the activator concentration as a parameter, and permits a prediction of scintillation efficiency as a function of both dE/dx and concentration. The low scintillation efficiency to electrons is predicted as a consequence of the smaller recombination probability for particles of very low dE/dx. Finally, for a low-dE/dx particle in a crystal of 0.1 mole percent activator concentration, the diffusion length of energy carriers is found to be of order 20 A.

BLANC'S LAW—ION MOBILITIES IN HELIUM-NEON MIXTURES. Manfred A. Biondi* and Lorne M. Chanin,† Westinghouse Research Laboratories, Pittsburgh, Pennsylvania (Received December 19, 1960).

The mobilities of ions of near thermal energies are measured in helium-neon mixtures using a drift velocity apparatus. These studies permit the investigation of ion motion in gases, e.g., He^+ in Ne, under conditions where the charge transfer interaction is negligible compared to polarization attraction and short-range repulsion between ion and atom. In addition, the measurements provide a test of Blanc's empirical law, $1/\mu = f_1/\mu_1 + f_2/\mu_2$, which relates the mobility, μ, in a binary mixture to the pure gas mobilities, μ_1 and μ_2, and to the fractional gas concentrations, f_1 and f_2. A theoretical treatment developed by Holstein is presented which shows that deviations from Blanc's law are limited to a few percent. The mobilities of He^+, He_2^+, and Ne_2^+ ions are found to obey accurately Blanc's law. However, the "Ne^+" ion curve deviates markedly from the law. These deviations are explained in terms of the formation of moderately stable $(HeNe)^+$ ions from Ne^+. Finally, the observed mobilities of He_2^+ in Ne and Ne_2^+ in He are found to agree with the predictions of polarization theory.

*Visiting Professor of Physics at the University of Pittsburgh, Pittsburgh, Pennsylvania.

†Now at Minneapolis-Honeywell Research Center, Hopkins, Minnesota.

NUCLEAR INTERACTIONS IN DEUTERIUM FLUORIDE. H. Mark Nelson,* John A. Leavitt,† Milton R. Baker, and Norman F. Ramsey, Harvard University, Cambridge, Massachusetts (Received December 27, 1960).

The deuteron and fluorine magnetic resonance spectra in the molecule DF have been studied using the molecular beam method. The observed resonance patterns have been compared with those calculated on a UNIVAC computer. The parameters of the calculation were adjusted

until the theoretical and the experimental curves matched. In this manner the spin-rotational interaction constant of fluorine in DF was assigned the value $|c_F| = 160 \pm 1$ kc/sec and the quadrupole coupling constant of the deuteron in DF was assigned the value $|d_2| = 34 \pm 4$ kc/sec, which corresponds to $|eqQ/h| = 340 \pm 40$ kc/sec.

*Present address: Brigham Young University, Provo, Utah.

†Present address: University of Arizona, Tucson, Arizona.

NUCLEAR RESONANCE FLUORESCENCE FROM THE 279-kev LEVEL OF Tl^{203} WITH AN ULTRACENTRIFUGE. B. I. Deutch and F. R. Metzger, Bartol Research Foundation of the Franklin Institute, Swarthmore, Pennsylvania (Received December 19, 1960).

Resonance fluorescence from the 279-kev level of Tl^{203} was studied with the centrifuge method. Assuming a total conversion coefficient $\alpha_T = 0.225$, a mean life $\tau_\gamma = (5.00 \pm 0.24) \times 10^{-10}$ sec was calculated from the resonance scattering measured at different source velocities. Combining this lifetime with the $B(E2)$ from Coulomb excitation, the absolute value of the mixing amplitude $\delta = (E2/M1)^{1/2}$ is $|\delta| = 1.31^{+0.24}_{-0.18}$. The angular distribution of the resonance radiation was found to be of the form $W(\theta) = 1 + (0.87 \pm 0.08) P_2(\cos\theta)$. This angular distribution, together with the range of absolute values of δ given above, fixes the sign of δ as positive. The range of δ values permitted by the angular distribution measurements is $\delta = +1.20^{+0.20}_{-0.12}$.

LIFETIME OF THE 279-kev STATE OF Tl^{203}. A. Schwarzschild and J. V. Kane, Brookhaven National Laboratory, Upton, New York (Received January 5, 1961).

The lifetime of the first excited state of Tl^{203} at 279 kev has been measured using the delayed coincidence technique. From analysis of the exponential decay observed with an electronic time to pulse-height converter, the mean life was determined to be $(4.05 \pm 0.08) \times 10^{-10}$ sec. The decay of this state was observed using sources of Hg^{203} and Pb^{203}, both sources yielding the same mean life within statistical errors. This value of the lifetime agrees very well with the recent determination by Deutsch and Metzger utilizing the resonance fluorescence method.

NUCLEAR SPIN AND MAGNETIC MOMENT OF 2.6-hr Mn^{56}. W. J. Childs, L. S. Goodman,* and L. J. Kieffer,† Argonne National Laboratory, Argonne, Illinois (Received December 23, 1960).

The atomic-beam magnetic-resonance technique has been used to examine the hyperfine structure of 2.6-hr Mn^{56}. The results obtained are $I = 3$, $|a| = 56.3924 \pm 0.0023$ Mc/sec, $|b| \leq 0.050$ Mc/sec, $g_J = 2.0012 \pm 0.0001$, and $\mu_I = +3.2402 \pm 0.0002$ nm. The value given for the nuclear magnetic dipole moment is deduced from the Fermi-Segrè relation and is therefore subject to correction for a possible hyperfine anomaly.

*Currently on leave as a Guggenheim Fellow at the University of Heidelberg, Heidelberg, Germany.

†Present address: National Bureau of Standards, Washington, D. C.

EXCITED STATES IN N^{14} FROM THE ELASTIC SCATTERING OF PROTONS BY C^{13}. E. Kashy,* R. R. Perry, R. L. Steele,† and J. R. Risser, Rice University, Houston, Texas (Received December 19, 1960).

Excited states in N^{14}* have been observed by measuring the differential elastic scattering cross section of $C^{13}(p,p)C^{13}$ for proton energies from 2.6 to 5.0 Mev. Resonances were observed at proton energies of 2.743, 2.87, 3.105, 3.20, 3.78, 3.980, 4.04, and 4.14 Mev, corresponding to excited states in N^{14} at 10.092, 10.21, 10.428, 10.52, 11.05, 11.240, 11.30, and 11.39 Mev, respectively. Single-level dispersion theory analysis indicates assignments $J^\pi = 1^+(2^+)$, 1^-, 2^+, 1^-, 1^+, 3^-, 2^-, and 1^+, respectively, for these states. Analysis of previously published $C^{13}(p,p)C^{13}$ data at lower energies confirms the assignments 1^-, 0^+, 0^-, 3^-, and 1^+ for the states at 8.05, 8.61, 8.75, 8.90, and 8.98 Mev. A resonance at 4.265 Mev corresponding to the known narrow state at 11.504 Mev was not found in the elastic scattering data although it was found to be strong in $C^{13}(p,p')C^{13}$*.

*Now at Department of Physics, Massachusetts Institute of Technology, Cambridge, Massachusetts.

†Now at Rocketdyne, Canoga Park, California.

GAMMA-RAY DE-EXCITATION OF THE LOW LEVELS OF F^{18}. J. A. Kuehner, E. Almqvist, and D. A. Bromley, Atomic Energy of Canada Limited, Chalk River Laboratories, Chalk River, Ontario, Canada (Received December 16, 1960).

The reaction $O^{16}(He^3,p)F^{18}$ has been employed to study the de-excitation gamma-ray branching of levels in F^{18} up to about 3 Mev using $p\gamma$ coincidence techniques. These measurements have been shown to be in reasonable agreement with tentative level identifications, 0 Mev (1+), 0.94 Mev (3+), 1.04 Mev (0+, $T=1$), 1.12 Mev (5+), 1.70 Mev (1+), 2.10 Mev (2+), 2.53 Mev (3+), and 3.06 or 3.13 Mev unresolved (2+, $T=1$), based on the intermediate-coupling shell-model predictions of Elliott and Flowers and of Redlich. An additional level at 1.08 Mev, which may arise from core excitation, is shown likely to have spin zero. It is suggested that the predicted energies need to be reduced by a factor of 0.6 and that the $T=1$ levels require shifting with respect to the $T=0$ levels to bring them into agreement with experiment. It has not been found possible to obtain an adequate fit to the F^{18} level spectrum presented in terms of a rotational collective model. The data may, however, be qualitatively in accord with an alpha-N^{14} cluster model interpretation. An example of the isotopic spin selection rule inhibiting $\Delta T=0$ $M1$ transitions in self-conjugate nuclei has been found.

$Si^{28}(d,p)Si^{29}$ REACTION. A. G. Blair* and K. S. Quisenberry, University of Pittsburgh, Pittsburgh, Pennsylvania (Received December 28, 1960).

The 15-Mev deuteron beam of the University of Pittsburgh cyclotron was used to study the $Si^{28}(d,p)Si^{29}$ reaction. Angular distributions of protons from most of the Si^{29} levels up to an excitation energy of 6.4 Mev were obtained. Good agreement with the 8-Mev deuteron results of Holt and Marsham (at a deuteron energy of 8 Mev) was found, except in a few cases where an $l=2$ distribution showed low-angle peaking in one of the experiments but not in the other. The angular distributions of the 5.94- and 6.19-Mev states in Si^{29}, not previously reported, were obtained. Butler curves with $l=2$ and $l=3$, respectively, were fitted to these two distributions. A somewhat unusual evaporation technique used to prepare the necessary targets from small quantities of SiO_2 with relatively high collection efficiency is described.

*Now at Los Alamos Scientific Laboratory, Los Alamos, New Mexico.

DECAY OF A NEW ISOTOPE, S^{30}. E. L. Robinson, J. I. Rhode, and O. E. Johnson, Physics Department, Purdue University, Lafayette, Indiana (Received December 19, 1960).

Scintillation techniques were used to study the beta and gamma radiation from high-purity natural silicon targets after irradiation with 8-Mev He^3 ions. In addition to activities associated with well-known radioisotopes, an activity with a (1.35 ± 0.10)-sec half-life was observed. A (677 ± 10)-kev gamma ray was associated with the 1.35-sec half-life. Decomposition of decay curves constructed from data obtained by observing annihilation radiation revealed a component with the same half-life. Half-life measurements using positrons with energies in excess of 3.15 Mev also indicated the presence of a 1.35-sec activity. The beta spectrum in coincidence with two annihilation quanta extended to ≈ 5.0 Mev, a higher energy than can be accounted for by positrons from the known reaction products. The beta spectrum in coincidence with the (677 ± 10)-kev gamma ray had an end-point energy of (4.30 ± 0.15) Mev. The assignment of the (1.35 ± 0.10)-sec activity to the decay of S^{30}, produced in the reaction $Si^{28}(He^3,n)S^{30}$, and the proposed decay scheme are supported by arguments formulated from the known characteristics of reaction products, half-life studies using both beta and gamma radiation, the features of the experimental beta and gamma spectra, beta-gamma coincidence spectra, nuclear systematics, and nuclear theory. The decay of the ground state of S^{30} takes place by at least two positron transitions: β_1, a (4.98 ± 0.15)-Mev superallowed transition to the 1+, $T=0$ ground state of P^{30}; β_2, a (4.30 ± 0.15)-Mev superallowed transition to the 0+, $T=1$ (0.677 ± 0.010)-Mev first excited state of P^{30}. No evidence was found for β_3, presumably an allowed transition to the 1+, (0.704 ± 0.005)-Mev second excited state of P^{30}, but an experimental upper limit of 25% is placed on its branching percentage. Branching percentages of (19 ± 2)%, (73 ± 7)%, and (8 ± 10)% for β_1, β_2, and β_3 were calculated using the measured S^{30} half-life, a S^{30}-P^{30} mass

difference of (6.01 ± 0.15) Mev, assumed charge independence of nuclear forces, and the fact that logft for 0+ to 0+ positron transitions within $T=1$ charge multiplets is almost constant.

LOW-LYING ENERGY STATES IN Ne^{20} FROM THE $F^{19}(d,n)Ne^{20}$ REACTION. R. E. Benenson,* H. Y. Chen, and L. J. Lidofsky, Columbia University, New York, New York (Received December 19, 1960).

Six neutron groups from the $F^{19}(d,n)Ne^{20}$ reaction corresponding to the lowest states in Ne^{20} have been observed at six angles of observation. The major part of the experiment employed nuclear emulsions and an average deuteron energy of 3.57 Mev. The importance of stripping appears to depend on the particular level involved; in particular, angular distributions leading to unambiguous assignments by stripping theory appear only for the ground, 1.63-Mev, and 6.75-Mev levels. The ground-state assignment appears to be energy dependent when the present $l_p=2$ value is compared to the $l_p=0$ value previously reported for a higher bombarding energy. The 4.25-Mev level in Ne^{20} gives rise to an angular distribution which could be either $l_p=2$ or $l_p=3$, but the fit to theory is not satisfactory for either case. A qualitative argument is given favoring the latter value. No assignment can be made to the 4.97- and 5.63-Mev levels.

A brief second experiment with a fast-neutron spectrometer was performed in order to obtain an absolute differential cross section at 0° for Ne^{20} left in its 6.75-Mev level. The reduced width obtained from this cross section is compared with a published reduced width for this same level obtained by elastic scattering of alpha particles by O^{16}.

*Permanent address: City College of New York, New York, New York.

EXCITED STATES IN P^{29} FROM THE SCATTERING OF PROTONS BY Si^{28}. T. A. Belote, E. Kashy,* and J. R. Risser, Rice University, Houston, Texas (Received December 28, 1960).

Excited states in P^{29} have been observed by measuring the differential elastic scattering cross section of $Si^{28}(p,p)Si^{28}$ for proton energies from 2.0 to 5.0 Mev and the differential inelastic scattering cross section of $Si^{28}(p,p')Si^{28*}$ ($Q=-1.78$ Mev) for proton energies from 3.0 to 5.2 Mev. Resonances were observed at 2.080, 2.88, 3.095, 3.334, 3.571, 3.710, 3.98, 4.235, 4.36, 4.43, and 4.884 Mev, corresponding to excited states in P^{29} at 4.732, 5.50, 5.711, 5.942, 6.171, 6.305, 6.57, 6.812, 6.93, 7.00, and 7.438 Mev, respectively. Single-level dispersion theory analysis indicates assignments $J^\pi = 1/2^+$, $1/2^-$, $5/2^-$, $3/2^+$, $3/2^-$, $1/2^-$, $1/2^+$, $3/2^+$, $1/2^+$, $1/2^-$, and $5/2^-$, respectively, for these states.

*Present address: Department of Physics, Massachusetts Institute of Technology, Cambridge, Massachusetts.

LEVELS IN N^{14} AT 11.74 AND 11.82 Mev. J. K. Bair, Oak Ridge National Laboratory, Oak Ridge, Tennessee (Received December 6, 1960).

The known angular distribution of the $C^{13}(p,p'\gamma)C^{13}$ 3.68-Mev gamma rays is not sufficient to uniquely determine the spin and parity of the 11.74-Mev N^{14} level for the case of arbitrary channel-spin mixing. To resolve this ambiguity the angular distribution of the inelastically scattered protons has been measured. Of the previous possibilities, $J^\pi = 1^+$, $2^\pm$, and 3^-, the assignment 1^+ is selected. A new level is found at 11.82 Mev in N^{14} having a width of about 100 kev, and decaying through the 3.09-Mev level in C^{13}. An angular distribution of the inelastically scattered protons from this new level shows strong interference effects.

(p,n) ANGULAR DISTRIBUTIONS FROM MIRROR NUCLEUS TARGETS: C^{13}, B^{11}, AND Be^9. R. D. Albert, S. D. Bloom, and N. K. Glendenning, Lawrence Radiation Laboratory, University of California, Livermore and Berkeley, California (Received December 27, 1960).

Neutron angular distributions from the (p,n) reactions in C^{13}, B^{11}, and Be^9 have been measured using a long-counter detection technique in conjunction with the Livermore 90-inch variable-energy cyclotron. Proton energies ranged from threshold (2.0 Mev to 3.2 Mev) up to 5.7 Mev. The aim here was to find qualitative experimental evidence bearing on the direct-reaction mechanism proposed by Bloom, Glendenning, and Moszkowski wherein the (p,n) reaction connecting the ground states of mirror

nuclei should go via a direct mode which is derived principally from the residual two-body interaction between the incoming proton and the bound neutron (or neutrons). It is found that the experimental evidence supports this hypothesis in that the angular distribution changes slowly in the direction of increasing complexity with increasing energy, largely ignoring the occurrence of resonances except in their immediate vicinity. Also a tentative grouping by pairs of the (p,n) angular distributions for (C^{13}, N^{15}) and (Be^{9}, B^{11}) shows marked similarities between the members of each pair in conformity with the twin-reaction picture stemming from the same theory. Finally, preliminary results are presented of an IBM 704 computation program using a distorted-wave Born approximation theory formulated originally by Glendenning. The comparison between theory and experiment, although based on early returns, is in general encouraging. It is found that a triplet-singlet interaction strength ratio is required here which is about 2/3 of that derived from the Gammel-Thaler phenomenological potential. However, in view of the basic differences between the free and the bound two-body problem it is felt that more knowledge will be required in order properly to compare the present results with the free-scattering analyses.

NEW ISOTOPE OF MANGANESE; CROSS SECTIONS OF THE IRON ISOTOPES FOR 14.8-Mev NEUTRONS. D. M. Chittenden, II, D. G. Gardner, and R. W. Fink,* Department of Chemistry, University of Arkansas, Fayetteville, Arkansas (Received October 10, 1960; revised manuscript received February 1, 1961).

Bombardment of iron enriched in Fe^{58} with 14.8-Mev neutrons produces an activity having a half-life of 1.1 ± 0.1 min. On the basis of cross bombardments and the gamma-ray spectrum of the activity, this is assigned to Mn^{58}. In addition, the following cross sections were measured: $Fe^{58}(n,p)$, 23.0 ± 3.5 mb; $Fe^{57}(n,p)$, 71.0 ± 7.0 mb; $Fe^{56}(n,p)$, 128 ± 13 mb; $Fe^{58}(n,\alpha)$, 21.5 ± 2.0 mb; $Fe^{54}(n,\alpha)$, 270 ± 135 mb; $Fe^{57}(n,np)$, 6.1 ± 2.6 mb; $Fe^{54}(n,2n)$, 7.9 ± 0.8 mb; $Fe^{54}(n,t)$, 0.6 ± 0.1 mb.

*Visiting scientist at Gustaf Werner Institute for Nuclear Chemistry, University of Uppsala, Uppsala, Sweden, 1959-1960.

DELAYED NEUTRONS FROM N^{17}. G. J. Perlow, W. J. Ramler, A. F. Stehney, and J. L. Yntema, Argonne National Laboratory, Argonne, Illinois (Received December 19, 1960).

The energy of the delayed neutrons which follow the decay of N^{17} has been measured by means of a triple proportional-counter recoil spectrometer. The N^{17} was obtained from the $C^{14}(\alpha,p)N^{17}$ reaction at a mean α-particle energy of 25 Mev. Two neutron groups were observed, with energies of 1.22 ± 0.06 Mev and 0.426 ± 0.018 Mev. These correspond to neutron emission from the $3/2^-$ states of O^{17} at 5.38 and 4.55 Mev, respectively. This result is consistent with the expected J^π of $1/2^-$ for the ground state of N^{17} and with the small stripping widths for these levels in $O^{16}(d,p)O^{17}$. The ratio of the intensity of the high-energy group to the low-energy one is 1.6, which corresponds to a ratio of 4 for the squares of the β-decay matrix elements.

CALCULATIONS IN NUCLEAR EVAPORATION THEORY. Richard Chasman, Argonne National Laboratory, Argonne, Illinois (Received July 28, 1960; revised manuscript received January 27, 1961).

Methods are developed for analytic treatment of problems in nuclear evaporation theory using the level density formula $\exp\{2[a(E^* - \epsilon)]^{1/2}\}$. Several useful expansions are given, with their ranges of validity. Comparisons made with existing calculations indicate the validity of this approach.

HIGH-ENERGY POTENTIAL SCATTERING WITH SHORT-RANGE FORCES. B. J. Malenka, Northeastern University, Boston, Massachusetts, and H. S. Valk, University of Nebraska, Lincoln, Nebraska (Received December 27, 1960).

An attempt is made to separate out long- and short-range effects for high-energy elastic scattering. Within the context of a high-energy approximation, expressions for the scattering amplitudes are obtained for the cases $kR \gg ka \gg 1$ and $kR \gg 1 > ka$, where R and a denote the long and short ranges, respectively. For the latter case, the entire short-range effect is included in a phenomenological S-wave term while the long-range contributions are written explicitly.

INTERPRETATION OF ELASTIC π^+-p SCATTERING AT 1.1 Bev. B. J. Malenka, Northeastern University, Boston, Massachusetts, and H. S. Valk, University of Nebraska, Lincoln, Nebraska (Received December 27, 1960).

Using a high-energy approximation, it is shown that the π^+-p elastic scattering data at 1.1 Bev can be interpreted in terms of coherent scattering produced by an absorptive Gaussian well having a root-mean-square range of the size of the proton charge radius plus a short-range interaction whose principal effect is presented phenomenologically as a contribution to the S wave.

METHOD OF DETERMINING THE SPIN AND PARITY OF A PION-HYPERON RESONANCE. Richard H. Capps, Northwestern University, Evanston, Illinois (Received December 22, 1960).

The reaction sequence, $M_1+N_1 \rightarrow Y^*+M_2$; $Y^* \rightarrow Y+\pi_1$; $Y \rightarrow N_2+\pi_2$ is considered, where M_1 and M_2 are spin-zero mesons, N_1 and N_2 are nucleons, Y is a Λ or Σ^+ particle, and Y^* is a pion-hyperon resonance of spin 1/2 or 3/2. The general form of the angular distribution of the particles π_1 and N_2 is written down under the assumption that final-state interactions between the meson M_2 and the Y^* decay particles may be neglected. If any polarization of the hyperon Y exists, the spin and parity of the resonance Y^* may be determined from this angular distribution. The structure of the spin density matrix of the Y^* is discussed.

SCATTERING OF 2-Bev/c MUONS IN CARBON AND LEAD. G. E. Masek, L. D. Heggie, Y. B. Kim, and R. W. Williams, Department of Physics, University of Washington, Seattle, Washington (Received November 23, 1960).

The scattering cross section of high-energy μ mesons in carbon and lead has been measured, using a pure, monoenergetic beam of muons obtained with the Bevatron at the Lawrence Radiation Laboratory. Preparation, purification, and measured properties of the beam are described. The median momentum was 2.00 ± 0.03 Bev/c, the spread in momentum was not more than $\pm 3.5\%$, and the effective contamination due to pions was 4.9×10^{-6}. During the experiment the total number of muons incident on the apparatus was 2.5×10^7. Counter hodoscopes recorded the muons scattered from 14.4 g/cm^2 of lead and from 27 g/cm^2 of carbon. Inelastic as well as elastic processes were accepted. Scattered particles were observed at angles up to 12° (momentum transfer ~400 Mev/c). The lead data cover the same range as those cosmic-ray experiments which have appeared to indicate an anomalously large scattering. No anomaly is found; the lead scattering agrees closely with the distribution calculated by Cooper and Rainwater for purely electromagnetic interactions. The carbon data permit a better comparison with theoretical expectations, since one is measuring the single-scattering cross section directly, and one can account for the effects of nuclear structure rather accurately, using electron-scattering data and a detailed theoretical analysis of Drell and Schwartz. The carbon scattering results, based on 300 events in the region 70 Mev/c - 400 Mev/c momentum transfer, agree closely with the Drell-Schwartz theory. The upper limits which this result places on a nonelectromagnetic scattering cross section and on a muon form factor are discussed.

π^+-p ELASTIC SCATTERING AT 310 Mev: RECOIL-NUCLEON POLARIZATION. James H. Foote,* Owen Chamberlain, Ernest H. Rogers, Herbert M. Steiner, Clyde E. Wiegand, and Thomas Ypsilantis, Lawrence Radiation Laboratory, University of California, Berkeley, California (Received December 27, 1960).

The recoil-proton polarization in π^+-p elastic scattering at 310-Mev incident-pion laboratory kinetic energy has been experimentally measured at four scattering angles with scintillation counters. Polarization values obtained, related rms experimental errors, and mean center-of-mass recoil angles are $+0.044 \pm 0.062$ at 114.2 deg, -0.164 ± 0.057 at 124.5 deg, -0.155 ± 0.044 at 133.8 deg, and -0.162 ± 0.037 at 145.2 deg. The sign of the polarization is defined to be positive when a preponderance of the recoil protons had their spin vectors pointing in the direction of $\vec{p}_i \times \vec{p}_f$, where this quantity is the cross product of the initial and final momentum vectors of the conjugate pions. A beam of 1×10^6 pions per sec incident upon a 1.0-g/cm^2-thick liquid-hydrogen target produced the recoil pro-

tons, which were then scattered by a carbon target at a mean energy varying with recoil angle from 113 to 141 Mev. The polarization of the recoil protons was analyzed by measuring the asymmetry produced in the carbon scattering. A proton beam of known polarization was used to determine the analyzing ability (measured asymmetry divided by the polarization of the incident protons) of the system at each recoil angle. Values obtained for the analyzing ability range from 0.41 to 0.57.

*Now at Lawrence Radiation Laboratory, Livermore, California.

π^+-p ELASTIC SCATTERING AT 310 Mev: PHASE-SHIFT ANALYSIS. James H. Foote,* Owen Chamberlain, Ernest H. Rogers, and Herbert M. Steiner, Lawrence Radiation Laboratory, University of California, Berkeley, California (Received December 27, 1960).

A comprehensive phase-shift analysis of π^+-p elastic-scattering data at 310-Mev incident-pion laboratory kinetic energy has been performed. The experimental data utilized include measurements of the differential and total cross sections and of the recoil-proton polarization. The D-wave phase shifts were found to be definitely needed in order to attain an adequate fit to the data. A general search for phase-shift solutions was carried out, using S-, P-, and D-wave phase shifts. One solution—of the Fermi type—was found that fits the data significantly better than any of the other solutions obtained. The calculated errors in the phase shifts of this set vary from 0.4 to 0.6 deg. Because it was felt that these errors might be deceivingly restrictive, the effects of small nuclear F-wave phase shifts on the results of the analysis were investigated and were found to be large; not only are the uncertainties in the original Fermi-type solution increased, but additional sets of phase shifts arise that fit the data well. One of these new solutions is similar to the original Fermi set except that the magnitudes of the phase shifts is this new fit are in general larger than those in the initial solution, and the signs of the D-wave phase shifts are reversed. The nuclear phase shifts in the original Fermi solution and their rms errors are (when F-wave phase shifts are allowed): $S_{3,1} = -17.2 \pm 2.6$ deg, $P_{3,1} = -2.9 \pm 4.0$ deg, $P_{3,3} = 135.0 \pm 0.6$ deg, $D_{3,3} = 3.1 \pm 2.6$ deg, $D_{3,5} = -4.9 \pm 2.1$ deg, $F_{3,5} = 0.5 \pm 0.6$ deg, $F_{3,7} = -0.6 \pm 1.4$ deg. Although theory appears to favor this set, further theoretical and experimental evidence is desirable. The values given here for the first five phase shifts approximate the corresponding values obtained when the F-wave phase shifts were assumed negligible. However, all except $P_{3,3}$ fall outside the limits set by the small original errors. Inelastic-scattering processes were neglected during the phase-shift analysis. Calculations indicate that, if these processes could properly be taken into account, any changes in the quoted values of the phase shifts would probably be well within the corresponding errors given here. Extension of the phase-shift inquiries to include G waves was attempted, but it was observed that the available data and theory do not allow the G-wave interaction to be significantly incorporated into the analysis.

*Now at Lawrence Radiation Laboratory, Livermore, California.

COORDINATE INVARIANCE AND ENERGY EXPRESSIONS IN GENERAL RELATIVITY. R. Arnowitt, S. Deser, and C. W. Misner,* Brandeis University, Waltham, Massachusetts, and Syracuse University, Syracuse, New York (Received December 2, 1960).

The invariance of various definitions proposed for the energy and momentum of the gravitational field is examined. We use the boundary conditions that $g_{\mu\nu}$ approaches the Lorentz metric as $1/r$, but allow $g_{\mu\nu,\alpha}$ to vanish as slowly as $1/r$. This permits "coordinate waves." It is found that none of the expressions giving the energy as a two-dimensional surface integral are invariant within this class of frames. In a frame containing coordinate waves they are ambiguous, since their value depends on the location of the surface at infinity (unlike the case where $g_{\mu\nu,\alpha}$ vanishes faster than $1/r$). If one introduces the prescription of space-time averaging of the integrals, one finds that the definitions of Landau-Lifshitz and Papapetrou-Gupta yield (equal) coordinate-invariant results. However, the definitions of Einstein, Møller, and Dirac become unambiguous, but not invariant.

The averaged Landau-Lifshitz and Papapetrou-Gupta expressions are then shown to give the correct physical energy-momentum as determined by the canonical formulations Hamiltonian involving only the two degrees of freedom of the field. It is shown that this latter definition

yields that inertial energy for a gravitational system which would be measured by a nongravitational apparatus interacting with it. The canonical formalism's definition also agrees with measurements of gravitational mass by Newtonian means at special infinity. It is further shown that the energy-momentum may be invariantly calculated from the asymptotic form of the metric field at a fixed time.

*On leave from Palmer Physical Laboratory, Princeton University, Princeton, New Jersey.

CHARGED-SCALAR STRONG-COUPLING THEORY FOR TWO-NUCLEON SYSTEM. K. W. Chun, Department of Physics, Columbia University, New York, New York (Received December 22, 1960).

The Serber-Pais charged-scalar strong-coupling method is extended to the two-nucleon system. It is shown explicitly that, whereas the nuclear force depends on the renormalized coupling constant alone at the large internucleon separations, its dependence on the unrenormalized coupling constant alone becomes increasingly pronounced as the two nucleons come closer together.

CONSTRUCTION OF UNITARY SCATTERING AMPLITUDES. R. Blankenbecler, Palmer Physical Laboratory, Princeton University, Princeton, New Jersey (Received December 22, 1960).

A general linear technique is discussed which constructs unitary scattering amplitudes without expanding in partial waves and in the presence of inelastic channels. Two- and three-particle intermediate states are discussed explicitly, but the method can be extended directly to any finite number of particles.

A new approximation technique suggested by this formalism is applied to electroproduction of pions from pions and pion–K-meson scattering. A form of the impulse approximation is derived for both the coupled form factor and the coupled scattering amplitude problems. The nucleon and deuteron form factor system is briefly discussed.

Finally, a model field theory which contains three-particle intermediate states is formulated and solved by the linear technique for purely pedagogical reasons.

SELF-CONSISTENT FIELD THEORY OF NUCLEAR SHAPES. Michel Baranger, Carnegie Institute of Technology, Pittsburgh, Pennsylvania (Received December 27, 1960).

The Hartree-Fock equations are generalized to include pairing effects on the same footing with field-producing effects. In addition to the Hartree potential, there enters a pairing potential. When applied to a spherically symmetric shell-model Hamiltonian, these equations may possess deformed solutions. Application is made to pairing plus quadrupole forces, with results identical to those of Belyaev and Kisslinger and Sorensen. The spherical shape becomes unstable when some collective vibration of the spherical nucleus reaches zero frequency.

NOTE ON THE MODIFIED GRAVITATIONAL EQUATIONS $g^2R_{ik}=0$. Daniel M. Lipkin, 6 Sealey Avenue, Hempstead, New York (Received August 29, 1960; revised manuscript received January 9, 1961).

The single example of a gravitational manifold which Einstein and Rosen presented in support of their modified field equations $g^2R_{ik}=0$ is shown to satisfy uniformly the unmodified field equations $R_{ik}=0$ and hence to provide insufficient logical support for their proposed modification. The demonstration is made in the original coordinates used by Einstein and Rosen, by direct calculation of the curvature tensor of the manifold.